



Future river flows and flood extent in the Upper Niger and Inner Niger Delta: GCM-related uncertainty using the CMIP5 ensemble

Julian R. Thompson, Andrew Crawley & Daniel G. Kingston

To cite this article: Julian R. Thompson, Andrew Crawley & Daniel G. Kingston (2017) Future river flows and flood extent in the Upper Niger and Inner Niger Delta: GCM-related uncertainty using the CMIP5 ensemble, Hydrological Sciences Journal, 62:14, 2239-2265, DOI: [10.1080/02626667.2017.1383608](https://doi.org/10.1080/02626667.2017.1383608)

To link to this article: <http://dx.doi.org/10.1080/02626667.2017.1383608>



© 2017 The Author(s). Published by Informa UK Limited, trading as Taylor & Francis Group.



Published online: 12 Oct 2017.



[Submit your article to this journal](#)



Article views: 240



[View related articles](#)



[View Crossmark data](#)



Citing articles: 1 [View citing articles](#)

Future river flows and flood extent in the Upper Niger and Inner Niger Delta: GCM-related uncertainty using the CMIP5 ensemble

Julian R. Thompson^a, Andrew Crawley^a and Daniel G. Kingston^b

^aWetland Research Unit, UCL Department of Geography, University College London, London, UK; ^bDepartment of Geography, University of Otago, Dunedin, New Zealand

ABSTRACT

A semi-distributed hydrological model of the Upper Niger and the Inner Niger Delta is used to investigate the RCP 4.5 scenario for 41 CMIP5 GCMs in the 2050s and 2080s. In percentage terms, the range of change in precipitation is around four times as large as for potential evapotranspiration, which increases for most GCMs over most sub-catchments. Almost equal numbers of sub-catchment–GCM combinations experience positive and negative precipitation change. River discharge changes are equally uncertain. Inter-GCM range in mean discharge exceeds that of precipitation by three times in percentage terms. Declining seasonal flooding within the Inner Delta is dominant; 78 and 68% of GCMs project declines in October and November for the 2050s and 2080s, respectively. The 10- and 90-percentile changes in mean annual peak inundation range from -6136 km^2 (-43%) to $+987 \text{ km}^2$ ($+7\%$) for the 2050s and -6176 km^2 (-43%) to $+1165 \text{ km}^2$ ($+8.2\%$) for the 2080s.

ARTICLE HISTORY

Received 25 August 2016
Accepted 7 August 2017

EDITOR

M.C. Acreman

ASSOCIATE EDITOR

S. Kanae

KEYWORDS

Inner Niger Delta; climate change; uncertainty; hydrological modelling; CMIP5

Introduction

Hydrological processes are key drivers within wetland environments (e.g. Baker *et al.* 2009). A wetland's water level regime exerts a dominant influence upon wetland vegetation, animals and biogeochemical processes. In turn, the ecosystem services provided by wetlands are conditioned by the interplay between hydrological, biophysical and ecological processes (Maltby *et al.* 2011). In some locations these wetland ecosystem services are central to the livelihoods of large human populations, a role that is clearly demonstrated in Africa's floodplains. Seasonal flooding supports agriculture, grazing and fisheries, provides water for domestic use either directly or through aquifer recharge, and sustains biodiversity that is often of international importance (Drijver and Marchand 1985, Adams 1992, Thompson and Polet 2000; Rebello *et al.* 2010). Africa's floodplains therefore typify the ecological, economic and social significance of "wetlands in drylands" (Scoones 1991). Despite this significance, many African floodplains have experienced changes in flooding patterns due to water resource developments, in particular dams. These changes have in turn impacted the provision of ecosystem services and the people that depend upon them (e.g. Thompson and Hollis 1995, Barbier and Thompson 1998, Lemly *et al.* 2000, Mumba and Thompson 2005, Kingsford *et al.*

2006). Further modifications to the hydro-ecological conditions of Africa's floodplain wetlands are likely to result from climate change.

Intensification of the global hydrological cycle will have major implications for catchment hydrological processes (Kundzewicz *et al.* 2007, Bates *et al.* 2008; IPCC 2014). Modifications to precipitation and evapotranspiration will impact runoff, river flow and groundwater recharge, with the nature of these changes varying around the globe (Arnell and Gosling 2013). Shifts in the magnitude and timing of flows into and out of wetlands will alter wetland water level regimes and flooding patterns (Ramsar Bureau 2002, Acreman *et al.* 2009, Singh *et al.* 2010, Thompson *et al.* 2017a), with consequent impacts on their ecological character and ecosystem service delivery (Erwin 2009, Thompson *et al.* 2009, Singh *et al.* 2011). Hydrological models have been widely used to assess the impacts of climate change upon a range of wetlands (e.g. Candela *et al.* 2009, Thompson *et al.* 2009, Singh *et al.* 2010, Barron *et al.* 2012, Carroll *et al.* 2015, House *et al.* 2016). This is commonly undertaken by forcing meteorological inputs to a previously calibrated model with climate projections from General Circulation Models (GCMs) that have themselves been forced with greenhouse gas emissions scenarios.

Each stage of such a climate change impact assessment is associated with uncertainties (Gosling *et al.*

2011), leading to what has been described as a “cascade of uncertainty” (Schneider 1983, Wilby and Dessai 2010). Uncertainty is associated with future emissions scenarios, whilst different GCMs often produce different projections for the same scenario. Additional uncertainty is due to the downscaling of GCM projections for use in hydrological models. An individual hydrological model may be subject to uncertainty due to imprecise knowledge of hydrological system behaviour compounded by incomplete or erroneous hydro-meteorological data (e.g. Van Dijk *et al.* 2008), whilst alternative hydrological models that give similar results for a historical baseline period may respond differently when forced with GCM projections for the same climate change scenario (Chiew *et al.* 2008, Gosling and Arnell 2011, Haddeland *et al.* 2011, Thompson *et al.* 2013). Translating hydrological changes to ecological responses within wetlands relies on knowledge of the requirements of individual species and communities as well as hydrological controls upon ecosystem services. These relationships are often uncertain, as are the potential management responses to climate change-related modification to catchment and wetland hydrology.

A number of studies have demonstrated that the most significant source of uncertainty is often GCM-related uncertainty (e.g. Graham *et al.* 2007, Prudhomme and Davies 2009, Gosling *et al.* 2011, Thompson *et al.* 2013, 2014a, 2014b, Green *et al.* 2014). These earlier studies include assessments of uncertainty on future river flows within West Africa’s Upper Niger Basin and in turn the impacts upon seasonal inundation within one of the region’s largest floodplain wetlands, Mali’s Inner Niger Delta (Thompson *et al.* 2016). A hydrological model of the basin and Inner Delta was forced with projections from a relatively small ensemble of GCMs for a 2°C increase in global mean temperature. Of the seven GCMs investigated, six produced declines in annual river inflow to the Inner Delta, although these varied in magnitude from less than 1% to over 50%. Results for the remaining GCM suggested small (<5%) increases in river inflows. Changes in peak seasonal flood extent varied from a mean increase of just over 10%, through almost negligible declines, to reductions of nearly 60%. Although these results indicated a substantial possible range in river flow and seasonal flood extent, the small ensemble of GCMs limited the opportunity for assessment of the most likely direction of change. Like many of the earlier studies, the climate change projections adopted by Thompson *et al.* (2016) were derived from the previous generations of climate models and emissions scenarios, rather than those of the more recent Coupled Model Intercomparison Project Phase 5 (CMIP5) and Representative Concentration Pathway (RCP) scenarios.

The CMIP5 ensemble is significantly larger than those of previous generations of GCMs, providing enhanced opportunities to assess GCM-related uncertainty (Knutti and Sedlacek 2013). The current study therefore expands the investigation of GCM-related uncertainty for the Upper Niger and the Inner Niger Delta using 41 CMIP5s GCMs and the RCP 4.5 scenario.

Methods

The Upper Niger and the Inner Niger Delta

The catchment upstream of the Inner Delta comprises the Upper Niger (147 000 km²), which rises in the Fouta Djallon highlands of Guinea, and the Niger’s major tributary, the Bani (129 000 km²), whose headwaters are in the Ivory Coast (Fig. 1, Zwarts *et al.* 2005a). The Inter-Tropical Convergence Zone controls the climate of the region and, in turn, the hydrological characteristics of its rivers (Drijver and Marchand 1985, Adams 1992, Thompson 1996). Precipitation is highly seasonal and peaks in August. The duration of the annual wet season varies from 8 months (March–October) over the southwest part of the basin to 3 months (July–September) over the Inner Niger Delta. The intervening dry period is characterized by very little or no rainfall. Annual rainfall also displays a similar southwest–northeast gradient. Mean annual totals vary from around 2100 mm over the headwaters of the Niger, through 1500 mm in the Upper Bani to around 250 mm over the downstream parts of the Inner Delta (Thompson *et al.* 2016). Inter-annual variability in precipitation across the Upper Niger is large, with a decline since the 1970s being widely reported (e.g. Zwarts *et al.* 2005a, Mahé 2009, Louvet *et al.* 2011). Spatial variation in potential evapotranspiration (PET) is in the opposite direction to precipitation; annual PET over the Inner Niger Delta is around 2150 mm, whilst in the far southwest it is approximately 1800 mm.

Flows in the basin’s rivers are highly seasonal and, like precipitation, exhibit large inter-annual variability with a dominant declining trend since the 1970s. The magnitude of these declines is larger than that experienced by precipitation (Louvet *et al.* 2011), likely reflecting reduced baseflow in response to cumulative reductions in rainfall (Mahé 2009). Upstream of the Inner Niger Delta discharges begin to rise with the rains and peak in September (Zwarts *et al.* 2005a). Discharges subsequently decline, with the lowest flows occurring in March–May. The annual flood takes 3–4 months to pass through the Inner Delta and consequentially discharges downstream peak in November or December (Sutcliffe and Parks 1989, John *et al.*

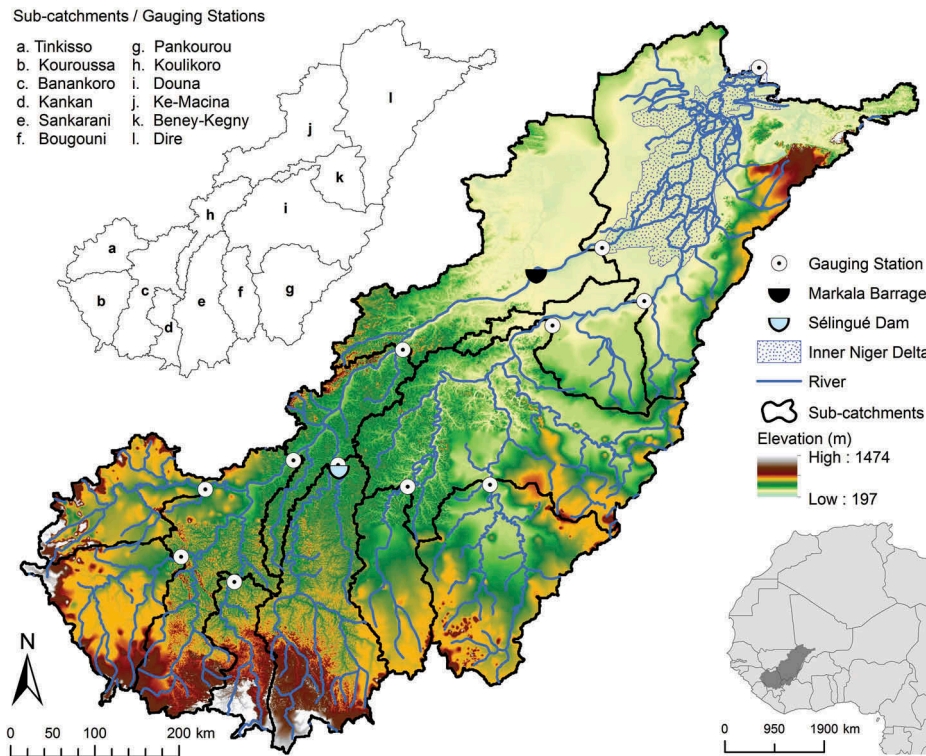


Figure 1. The Upper Niger Catchment and the Inner Niger Delta. The sub-catchments and their downstream gauging stations for which separate sub-models were developed are indicated.

1993). The period of high flows lengthens from 2–3 months upstream to 7 months downstream (Zwarts *et al.* 2005a). Flow magnitudes are reduced considerably due to evaporation from extensive flooding and seepage beneath inundated areas (Beadle 1974, Zwarts *et al.* 2005a). Mahé *et al.* (2009) estimated that the mean annual loss was around 40%, although this varied by between 24 and 48% over the period 1924–1996. Large losses occur when flooding is extensive (Zwarts and Grigoras 2005, Mahé *et al.* 2009). These losses are much smaller during drier periods, when inflows decline dramatically and flood extent is much reduced (Mahé *et al.* 2011b).

The lowest water levels within the Inner Niger Delta occur between May and July (e.g. Bergé-Nguyen and Crétaux 2015). At this time the area of permanent standing water is less than 4000 km² and can be very small in the driest years (Sutcliffe and Parks 1989, Zwarts and Grigoras 2005). As the annual flood enters the Delta, water levels rise with peak inundation occurring in October/November (Grove 1985, Crétaux *et al.* 2011). Peak flood extent shows large inter-annual variability. Zwarts and Grigoras (2005) employed a relationship between water levels and Landsat remote sensing-derived flood extent to show that peak inundation between 1956 and 2000 varied from only 8000 km² during the droughts of the 1980s to more than

24 000 km² in the 1950s. Estimates of flood extent for the last decade of this period correspond well with those established by Mariko *et al.* (2003) and Mariko (2004) using AVHRR remote sensing data.

The extensive floodplains of the Inner Niger Delta are extremely productive. In common with other African floodplains (e.g. Adams 1992, Thompson and Polet 2000), flood patterns exert a dominant influence on ecological conditions. Vegetation zonation is largely controlled by water depth and its seasonal variations (Zwarts *et al.* 2005b), whilst peak flood level and flood duration regulate fish recruitment and survival through the following dry season (Welcomme 1986, Zwarts and Diallo 2005). Although most large wild grazers and other large mammals such as hippo and manatee have been lost, the Inner Delta is still a biological hot-spot, especially for birdlife. It is one of the world's largest Ramsar sites. Populations of 28 waterbird species exceed 1% of the total flyway population, the threshold for recognition as internationally important (Van der Kamp *et al.* 2005). Over 1 million people utilize floodplain resources, so the Inner Delta has tremendous economic and social significance (Zwarts and Kone 2005a). The floodplains support agriculture, in particular rice cultivation, fishing and the grazing of cows, sheep and goats (Goosen and Kone 2005, Zwarts and Diallo 2005, Zwarts and Kone 2005b).

There are a number of water resources schemes within the river basin which have varying impacts on river flow and, in turn, flood extent. The Sotuba hydropower dam, constructed in 1929 on the Niger below Bamako, has a small reservoir and limited hydrological effects. The larger Sélingué Dam (1982) is on the Sankarani River (Fig. 1). Zwarts *et al.* (2005a) suggested that it reduces peak flows in the Niger at Ke-Macina by 10–20% and 20–30% in wet and dry years, respectively. Dry season releases are significant and sustain downstream flows with water being used for irrigation (Hassane *et al.* 2000). Water is diverted by the Markala Barrage from the River Niger for irrigation on the Office du Niger project (740 km² compared to the planned 9600 km²). These diversions are a small percentage of flows in the wet season, but dry season diversions can reduce flows in the Niger by half (Zwarts *et al.* 2005a). The Talo Dam on the Bani was constructed in 2006, beyond the end of the simulation period considered in the current study, whilst there are plans for future dams, including the Fomi hydropower dam on the Niandan above Kankan, which are likely to further impact downstream river flows (Zwarts *et al.* 2005a, Liéno *et al.* 2010).

The hydrological model

Thompson *et al.* (2016) provided a detailed account of the semi-distributed, conceptual hydrological model of the Upper Niger and Inner Delta, which is therefore only summarized here. The model was implemented in the STELLA systems modelling software (Version 10, iSee systems), which has been used in a number of hydrological modelling studies (e.g. Zhang and Mitsch 2005, Voinov *et al.* 2007, Ho *et al.* 2016). Using the approach employed by Ho *et al.* (2016), separate sub-models were developed for 11 sub-catchments defined by gauging stations at their downstream outlets (Fig. 1). Each sub-catchment model comprised reservoirs representing soil, groundwater and channel stores, and the water balance for each reservoir was evaluated at a monthly time step. Meteorological inputs/outputs to the soil store were specified as sub-catchment averaged monthly precipitation and PET totals, both multiplied by sub-catchment area. Precipitation was derived from the CRU TS 3.0 dataset (Mitchell and Jones 2005), whilst Hargreaves PET (Hargreaves and Samani 1982) was calculated using minimum, mean and maximum temperature from CRU TS 3.0 and extra-terrestrial solar radiation based on latitude. Actual evapotranspiration was limited by available soil storage. Overland flow from the soil store to the channel store was evaluated as any excess soil storage above a maximum storage capacity. Throughflow from the soil store to the channel store

and percolation from the soil store to the groundwater store were simulated using linear reservoir constants when threshold soil storage was exceeded. The same approach was used for baseflow from the groundwater store to the channel store. River discharge was simulated as the product of channel store and a reservoir constant. Simulated discharge volumes were evenly distributed through the month for comparison with observed mean monthly discharges. The model incorporated elements to represent Sélingué Dam and the Markala Barrage, the two largest dams operational during the modelled period or part thereof. As detailed by Thompson *et al.* (2016), these were based on previous analysis of their impacts upon river flow provided by Zwarts *et al.* (2005a).

The volume of water and, in turn, flood extent within the Inner Niger Delta was simulated in another sub-model replicating approaches used in previous models of this and other African floodplains (Sutcliffe and Parks 1987, 1989, Hollis and Thompson 1993a, 1993b, Thompson 1995, Thompson and Hollis 1995). The hydrological model provided river inflows from the Niger at Ke-Macina and the Bani at Beney-Kegny. River outflows were established using a relationship between mean monthly discharge below the Inner Delta at Douna and weighted aggregate inflows of the combined mean monthly discharges at Ke-Macina and Beney-Kegny during the four most recent months. River inflows were supplemented by direct precipitation onto the inundated area, based on the product of CRU TS 3.0 precipitation for grid cells covering the Inner Niger Delta and flood extent. The latter was based on a synthetic volume/area relationship which was subject to calibration. Evapotranspiration was simulated as the product of Hargreaves PET (calculated using the CRU TS 3.0 cells covering the Inner Delta) and the inundated area. This area was also multiplied by an infiltration rate to simulate seepage beneath the inundated area, a process that can be particularly significant during the flood period (Mahé *et al.* 2009).

The complete simulation period employed by Thompson *et al.* (2016) was 1950–2000, with the first half (1950–1975) being used for calibration and 1976–2000 for validation. Due to extended periods of missing data in the source Global Runoff Data Centre (GRDC) discharge records, model performance was also assessed for the central 1961–1990 period, which was used as a baseline for climate change assessment (repeated herein – see below). Model performance in reproducing observed discharges for all three periods was assessed using the Nash-Sutcliffe coefficient (NSE, Nash and Sutcliffe 1970), the Pearson correlation coefficient (r) and the bias (Dv; Henriksen *et al.* 2003).

Performance was classified using the scheme of Henriksen *et al.* (2008). Simulated peak annual flood extents within the Inner Niger Delta were compared with corresponding estimates provided by Zwarts and Grigoras (2005). These were available for 1956–2000, and were based on a relationship between water levels within the Delta and remote sensing-derived estimates of flood extents (a similar approach to that described by Mariko *et al.* (2003) and Mahé *et al.* (2011b)). As described by Thompson *et al.* (2016) the model performed very well for the calibration period, with Dv for river discharge being classified as “excellent” and “very good” for nine and three gauging stations, respectively. The NSE values were “excellent” for all but one gauging station. Whilst NSE values for the validation period were either “excellent” or “very good”, overestimation of seasonal peak discharges was common. Possible reasons for this overestimation include widespread declines in Sahelian vegetation cover in recent decades (Diello *et al.* 2005, Liéno *et al.* 2005, Leblanc *et al.* 2008), although these are more likely to increase runoff (Descroix *et al.* 2009, Amogu *et al.* 2010). Declining data quality and availability, widely reported in Sub-Saharan Africa (e.g. World Bank *et al.*, 1993, Giles 2005, Farquharson 2007, Pitman 2011), may also be a factor. These declines occurred just after the baseline period, so that discharge overestimation did not occur at this time. Values of both NSE and Dv were classified as “excellent” at nine stations and “very good” at three. During the calibration and baseline periods, model performance in terms of reproducing annual maxima flood extent was generally good, with peaks being overestimated by on average 3.3% for the former and underestimated by only 1.3% in the latter period. In both periods an approximately equal number of annual peaks were over- and underestimated. This was repeated for the validation period. Thompson *et al.* (2016) concluded that the performance of the model in replicating river discharge and flood extent, especially for the calibration and baseline periods, was sufficient to enable its use in climate change impact assessment.

Climate change scenarios

Revised meteorological inputs were derived for 41 CMIP5 GCMs (Table 1). The GCM results were obtained for the RCP 4.5 scenario (radiative forcing is stabilized at 4.5 W m^{-2} in the year 2100 without ever exceeding this value – Thomson *et al.* 2011) from the Royal Netherlands Meteorological Institute (KNMI) Climate Explorer (Trouet and Van Oldenborgh 2013). This particular RCP scenario was selected since it is considered an intermediate/mid-range emissions

scenario (Moss *et al.* 2010, van Vuuren *et al.* 2011) and has been used in other hydrological-based studies of GCM-related uncertainty (e.g. Dai 2012, Ho *et al.* 2016, Robinson 2017). In addition, the KNMI Climate Explorer provided results for the largest number of GCMs for the RCP 4.5 scenario. This multimodel approach incorporates both structural and parameter uncertainty by using a relatively large number of GCMs with different designs (Tebaldi and Knutti 2007). Ho *et al.* (2016) argued that, as results from more GCMs are employed, the degree of uncertainty should decline (Knutti *et al.* 2009), although this only applies when a sufficient number of GCMs are used. Following the approach of Ho *et al.* (2016), the delta factor method was used to derive revised sub-catchment precipitation and PET for two time slices: 2041–2070 (referred to as the 2050s) and 2071–2100 (the 2080s). Delta factors are widely used to provide scenarios suitable for hydrological modelling (e.g. Wilby and Wigley 1997, Thompson *et al.* 2009, Singh *et al.* 2010, Thompson 2012). The methodology is advantageous since scenario time series retain climate variability but are not affected by biases in a GCM’s simulation of it (Anandhi *et al.* 2011, Willems *et al.* 2012). It is, however, important to recognize that the approach does not represent projected changes in extremes or inter-annual variability (Diaz-Nieto and Wilby 2005).

Mean monthly maximum, mean and minimum temperatures as well as monthly precipitation totals were derived for each sub-catchment for the period 1961–1990 and each time slice. Monthly delta factors for both time slices ($^{\circ}\text{C}$ for temperature, % for precipitation) were derived at the sub-catchment scale. These were used to perturb the original CRU data and Hargreaves PET was re-evaluated using the new temperature time series. In addition, mean temperatures (maximum, mean and minimum) and precipitation were evaluated for each sub-catchment from all 41 GCMs. These were used to establish delta factors for the 2050s and 2080s and, in turn, to derive scenario precipitation and PET for an ensemble mean scenario using the methods described above. Empirical evidence suggests that such a multi-GCM ensemble mean for current conditions tends to agree more closely with observed climate data than a single GCM (Lambert and Boer 2001, Gillett *et al.* 2002, Palmer *et al.* 2005). According to this argument, the ensemble mean scenario should serve as a better indicator of the impacts of climate change than the results of one GCM. However, for this to be strictly valid the GCMs should be independent of each other (Pirtle *et al.* 2010). As described by Ho *et al.* (2016), institutions responsible

Table 1. CMIP5 GCMs used to produce climate change scenarios.

No	Model	Institution	GCM Group*
1	ACCESS1.0	Commonwealth Scientific and Industrial Research Organisation (CSIRO) and Bureau of Meteorology (BOM),	10
2	ACCESS1.3	Australia	10
3	BCC-CSM1.1	Beijing Climate Center, China Meteorological Administration	12
4	BCC-CSM1.1(m)		12
5	BNU-ESM	College of Global Change and Earth System Science, Beijing Normal University	12
6	CanESM2	Canadian Centre for Climate Modelling and Analysis	1
7	CCSM4	National Center for Atmospheric Research	12
8	CESM1(BGC)	Community Earth System Model Contributors	12
9	CESM1(CAM5)		12
10	CMCC-CM	Centro Euro-Mediterraneo per I Cambiamenti Climatici	11
11	CMCC-CMS		11
12	CNRM-CM5	Centre National de Recherches Météorologiques/Centre Européen de Recherche et Formation Avancée en Calcul Scientifique	11
13	CSIRO-Mk3.6.0	Commonwealth Scientific and Industrial Research Organisation in collaboration with Queensland Climate Change Centre of Excellence	2
14	EC-EARTH	EC-Earth consortium	11
15	FGOALS-g2	LASG, Institute of Atmospheric Physics, Chinese Academy of Sciences	3
16	FIO-ESM	The First Institute of Oceanography, SOA, China	12
17	GFDL-CM3	NOAA Geophysical Fluid Dynamics Laboratory	6
18	GFDL-ESM2G		6
19	GFDL-ESM2M		6
20	GISS-E2-H p1	NASA Goddard Institute for Space Studies	7
21	GISS-E2-H p2		7
22	GISS-E2-H p3		7
23	GISS-E2-H-CC		7
24	GISS-E2-R p1		7
25	GISS-E2-R p2		7
26	GISS-E2-R p3		7
27	GISS-E2-R-CC		7
28	HadGEM2-AO	Met Office Hadley Centre (additional HadGEM2-ES realizations contributed by Instituto Nacional de Pesquisas	10
29	HadGEM2-CC	Espaciais)	10
30	Had-GEM2-ES		10
31	INM-CM4	Institute for Numerical Mathematics	4
32	IPSL-CM5A-LR	Institut Pierre-Simon Laplace	8
33	IPSL-CM5A-MR		8
34	IPSL-CM5B-LR		8
35	MIROC5	Atmosphere and Ocean Research Institute (The University of Tokyo), National Institute for Environmental Studies, and Japan Agency for Marine-Earth Science and Technology	9
36	MIROC-ESM	Japan Agency for Marine-Earth Science and Technology, Atmosphere and Ocean Research Institute (The	9
37	MIROC-ESM-CHEM	University of Tokyo), and National Institute for Environmental Studies	9
38	MPI-ESM-LR	Max-Planck-Institut für Meteorologie (Max Planck Institute for Meteorologie)	11
39	MPI-ESM-MR	Meteorological Research Institute	11
40	MRI-CGCM3		5
41	NorESM1-M	Norwegian Climate Centre	12

*GCM groups are defined in Table 2.

for different GCMs share literature, parameter values and sections of model code (Abramowitz 2010), whilst the CMIP5 ensemble includes more than one GCM from an individual institution or more than one version of a given GCM (Table 1). In such cases, strict model independence is not achieved with, for example, results from institutions with multiple GCMs, having a greater influence over the ensemble mean. The potential for such biases to influence the ensemble mean can be addressed by grouping GCMs according to shared characteristics such as their atmospheric model (Hanel and Buishand 2015). Here the approach of Ho *et al.* (2016), which was inspired by the concept of model genealogy (Masson and Knutti 2011, Knutti *et al.* 2013), was used to identify 12 groups (Table 2) to which each of the 41 GCMs were assigned (see fourth column in Table 1). Five of these groups contained only one GCM whilst the remaining seven comprised

Table 2. CMIP5 GCM groups based on model genealogy.

No	Group name	Number of GCMs
1	CanESM2	1
2	CSIRO-Mk3.6.0	1
3	FGOALS-g2	1
4	INM-CM4	1
5	MRI-CGCM3	1
6	GFDL	3
7	GISS	8
8	IPSL	3
9	MIROC	3
10	UKMO	5
11	European	6
12	NCAR	8

between three and eight GCMs. Within an individual group, mean temperatures (maximum, mean and minimum) and precipitation were established for each sub-catchment and, using the approach described above, delta factors and, in turn, scenario precipitation and PET calculated for the 2050s and 2080s. A final

scenario, referred to here as the group ensemble mean, was established based on the mean temperatures and precipitation across the 12 groups. Subsequent sections provide results for the 41 GCMs and their ensemble mean, with the implications of grouping GCMs according to their genealogy being assessed separately.

Simulation of the climate change scenarios followed the approach used by Thompson *et al.* (2016). The two existing dams within the model (Sélingué Dam and Markala Barrage) were simulated as operational throughout the baseline (1961–1990) and scenario periods. Whilst this represented no change from the original calibrated model for the Markala Barrage, the Sélingué Dam was assumed to be in operation from the start of the baseline period instead of from 1982. In this way, differences between scenarios and the baseline can be attributed to changes in climate alone rather than a combination of dams and climate change. This approach assumes that the rainfall–runoff characteristics represented within the hydrological model remain stable in the future, an assumption widely employed in similar modelling studies in Africa (e.g. Ardoin-Bardin *et al.* 2009, Kingston and Taylor 2010) and elsewhere (e.g. Singh *et al.* 2010, Thompson *et al.* 2013).

Results

Scenario climate

Table 3 summarizes the impacts of the 41 CMIP5 GCMs upon mean annual precipitation and PET for the 2050s and 2080s. Baseline annual totals are shown for each model sub-catchment. Percentage changes in these totals are provided for the ensemble mean, the two extreme changes projected by individual GCMs and for a range of percentiles between 10 and 90%. The numbers of individual GCMs (and percentage of the 41 GCMs) in which precipitation and PET increase or decrease over each sub-catchment are also indicated. Scenario impacts over five representative sub-catchments are shown graphically in Figure 2 in the form of percentage changes in mean annual precipitation and PET. These are superimposed upon shaded bands that represent the percentile ranges employed in Table 3. The same bands are employed in Figure 3, which summarizes the impact of each scenario and the ensemble mean upon mean monthly precipitation and PET for the same representative sub-catchments.

Within all 12 sub-catchments, individual GCMs project both increases and decreases in mean annual precipitation (Table 3 and Fig. 2). Similar variability is demonstrated in the distribution of precipitation through the year (Fig. 3). The number of GCMs projecting increases in annual

precipitation over individual sub-catchments varies from 16 to 30 (2050s) and 15 to 29 (2080s). Out of the 492 sub-catchment–GCM combinations (12 sub-catchments \times 41 GCMs), precipitation increases in 276 (56.1%) for the 2050s and 259 (52.6%) for the 2080s. The inter-GCM range of change in mean annual precipitation varies considerably between different sub-catchments and increases between the 2050s and 2080s. There is some consistency in the GCMs responsible for the extreme changes with, for example, GCM 37 followed by GCM 36 (MIROC-ESM-CHEM and MIROC-ESM, respectively) dominating the largest increases in annual precipitation over eastern sub-catchments. At the other extreme, GCM 31 (INM-CM4) is associated with the largest reductions in 10 sub-catchments for the 2050s and in all 12 sub-catchments for the 2080s.

Beyond the most extreme changes, the 10–90-percentile range of change in annual precipitation for the 2050s varies between 13.6% (Sankarani – e) and 26.9% (Tinkisso – a). Across the 12 sub-catchments the mean range is 19.0%. The mean for the 2080s is 22.5% and the range varies between 15.6% (Sankarani – e) and 34.4% (Dire – l). The central 33% of changes (i.e. the 33–66-percentile range) has a mean range of 5.8% (4.2–9.5%, Sankarani (e) and Tinkisso (a), respectively) for the 2050s and 6.3% (4.2–11.5%, Dire (l) and Tinkisso (a), respectively) for the 2080s. Figure 3 demonstrates the small range in mean monthly precipitation for this central 33% of GCMs. In most cases the baseline falls within this range. For both time slices an equal number of sub-catchments experience increases and decreases in the 50-percentile change in annual precipitation (Table 3). Inter-sub-catchment variability is relatively small. On average very small increases in annual precipitation are projected (0.7 and 0.4% for the two time slices, respectively). Changes for the ensemble mean are similarly small (mean 1.1 and 1.3% for the 2050s and 2080s, respectively) although more sub-catchments experience increased annual precipitation (eight and nine, respectively). Mean monthly precipitation in each sub-catchment for the ensemble mean is very similar to the baseline (Fig. 3).

Annual PET increases for all GCMs in six of the 12 sub-catchments for both the 2050s and 2080s (Table 3 and Fig. 2). GCMs 36 and 37 project relatively small declines in the remaining sub-catchments, which are predominantly due to projected reductions in mean and especially maximum temperatures during the wet season. Declines in maximum temperature at this time of year are also projected by some other GCMs for some sub-catchments, leading to declines in wet season PET (Fig. 3). For the rest of the year monthly PET generally increases for all GCMs. GCMs 36 and 37 are clearly outliers compared to the other GCMs, and even then Table 3 and Figure 2

Table 3. Mean annual precipitation (Precip.) and potential evapotranspiration (PET) for the baseline (mm) and summary of changes from the 41 CMIP5 GCM climate change scenarios for sub-catchments within the Upper Niger catchment. E.M. indicates the changes (%) in annual totals for the ensemble mean, Max. and Min. represent the maximum and minimum changes (%) in annual totals, the corresponding figures for 90–10% represent the changes (%) in annual totals for the respective percentile (which define the shaded zones in Fig. 2). Shaded cells indicate negative changes compared to the baseline. +ve and -ve are the number (%) in brackets of GCMs in which scenario annual totals are above and below the baseline, respectively. Letters refer to the model sub-catchments indicated in Figure 1.

Parameter	Scenario	Sub-catchments											
		a	b	c	d	e	f	g	h	i	j	k	l
Precip. 2050	Baseline	1384.3	1677.0	1564.1	1730.2	1457.5	1282.6	1198.7	1056.3	957.8	585.2	740.7	446.1
	E.M.	-0.0	2.5	-1.3	2.6	1.9	-1.7	2.3	-1.3	2.3	0.1	0.0	6.1
	Max.	19.4	15.9	12.4	11.5	9.9	12.9	20.5	15.2	22.2	45.1	42.9	66.5
	90%	15.0	12.1	8.5	8.9	7.7	8.0	8.6	6.8	8.2	9.7	9.6	17.9
	66%	3.6	3.9	1.1	5.0	4.6	0.7	4.1	0.9	4.1	2.5	1.4	5.2
	50%	-2.3	2.2	-0.8	3.2	2.5	-1.4	3.5	-0.2	3.3	-2.6	-2.7	3.4
	33%	-6.0	-1.0	-4.8	0.1	0.2	-5.4	-0.6	-4.3	-0.1	-6.0	-5.8	0.7
	10%	-11.9	-6.8	-9.7	-5.2	-5.9	-10.3	-5.7	-10.0	-7.1	-13.1	-11.9	-8.8
	Min.	-22.6	-12.6	-15.9	-9.6	-11.1	-16.9	-12.9	-17.5	-13.5	-19.2	-18.8	-14.1
	+ve	18 (44)	26 (63)	19 (46)	29 (71)	29 (71)	18 (44)	27 (66)	19 (46)	28 (64)	16 (39)	17 (41)	30 (73)
-ve	23 (56)	15 (37)	22 (54)	12 (29)	12 (29)	23 (56)	14 (34)	22 (54)	13 (32)	25 (61)	24 (59)	11 (27)	
2080	E.M.	0.7	3.8	-1.7	3.4	2.4	-2.0	2.0	-1.4	1.9	0.1	0.0	6.3
	Max.	28.3	20.7	19.9	13.2	12.1	20.0	28.5	22.6	31.0	67.1	63.8	94.5
	90%	17.1	14.3	7.2	11.2	10.3	7.5	10.2	8.3	10.1	13.6	14.3	21.5
	66%	5.5	6.0	0.7	6.5	4.7	0.2	3.7	0.9	3.2	0.3	0.5	3.9
	50%	-1.3	3.8	-1.2	4.3	3.4	-1.5	2.5	-1.5	2.5	-4.3	-4.4	2.3
	33%	-6.0	-0.1	-5.2	0.3	0.3	-5.6	-1.4	-4.0	-1.6	-7.7	-7.7	-0.3
	10%	-13.2	-6.6	-12.4	-4.7	-5.3	-13.3	-7.2	-12.1	-8.3	-14.0	-14.1	-12.9
	Min.	-31.2	-20.7	-23.9	-16.4	-18.2	-24.6	-19.6	-26.2	-20.6	-27.7	-27.2	-22.4
	+ve	18 (44)	28 (68)	16 (39)	29 (71)	29 (71)	15 (37)	25 (61)	16 (39)	26 (63)	15 (37)	15 (37)	27 (66)
	-ve	23 (56)	13 (32)	25 (61)	12 (29)	12 (29)	26 (63)	16 (39)	25 (61)	15 (37)	26 (63)	26 (63)	14 (34)
PET 2050	Baseline	1883.9	1856.4	1920.7	1908.5	1924.3	1922.6	1924.2	1968.1	1969.7	2043.9	2015.3	2090.0
	E.M.	4.6	3.4	4.4	3.0	3.4	4.3	4.1	4.2	4.1	4.3	4.3	3.6
	Max.	8.2	7.4	8.6	6.5	6.6	8.6	7.6	8.4	7.6	8.3	8.3	7.2
	90%	6.8	5.4	6.1	5.5	5.6	6.1	6.2	6.0	6.1	5.9	5.9	5.7
	66%	5.6	4.3	5.3	4.3	4.6	5.2	4.9	5.1	4.9	4.9	4.9	4.5
	50%	4.8	3.3	4.8	3.7	3.9	4.7	4.3	4.6	4.2	4.5	4.6	3.4
	33%	4.0	2.3	4.0	2.4	3.1	3.9	3.4	3.9	3.4	4.1	4.1	3.2
	10%	2.0	1.3	1.9	1.7	1.8	1.8	1.7	1.7	1.7	1.6	1.6	1.1
	Min.	1.5	1.0	-2.3	-9.8	-7.7	-2.6	1.0	-2.5	1.0	0.4	0.4	-0.7
	+ve	41 (100)	41 (100)	39 (95)	39 (95)	39 (95)	39 (95)	41 (100)	39 (95)	41 (100)	41 (100)	41 (100)	39 (95)
-ve	0 (0)	0 (0)	2 (5)	2 (5)	2 (5)	2 (5)	0 (0)	2 (5)	0 (0)	0 (0)	0 (0)	2 (5)	
2080	E.M.	5.5	4.1	5.4	3.8	4.2	5.3	5.3	5.2	5.2	5.4	5.4	4.6
	Max.	10.1	7.6	10.6	8.5	8.7	10.6	9.7	10.4	9.6	10.4	10.5	9.1
	90%	8.7	7.0	8.6	6.8	7.4	8.6	8.2	8.4	8.1	8.1	8.2	7.8
	66%	6.7	5.2	6.5	5.1	5.4	6.4	6.1	6.3	6.1	5.9	6.0	5.2
	50%	5.8	4.1	5.8	4.1	4.6	5.7	5.3	5.6	5.3	5.5	5.6	4.7
	33%	3.9	2.8	4.4	2.9	3.3	4.3	4.1	4.2	4.1	4.9	4.9	4.0
	10%	2.6	1.7	2.3	2.3	2.5	2.2	2.2	2.1	2.2	2.2	2.1	1.7
	Min.	2.0	1.6	-1.6	-10.1	-7.5	-1.9	1.5	-1.8	1.5	0.3	0.3	-1.0
	+ve	41 (100)	41 (100)	39 (95)	39 (95)	39 (95)	39 (95)	41 (100)	39 (95)	41 (100)	41 (100)	41 (100)	39 (95)
	-ve	0 (0)	0 (0)	2 (5)	2 (5)	2 (5)	2 (5)	0 (0)	2 (5)	0 (0)	0 (0)	0 (0)	2 (5)

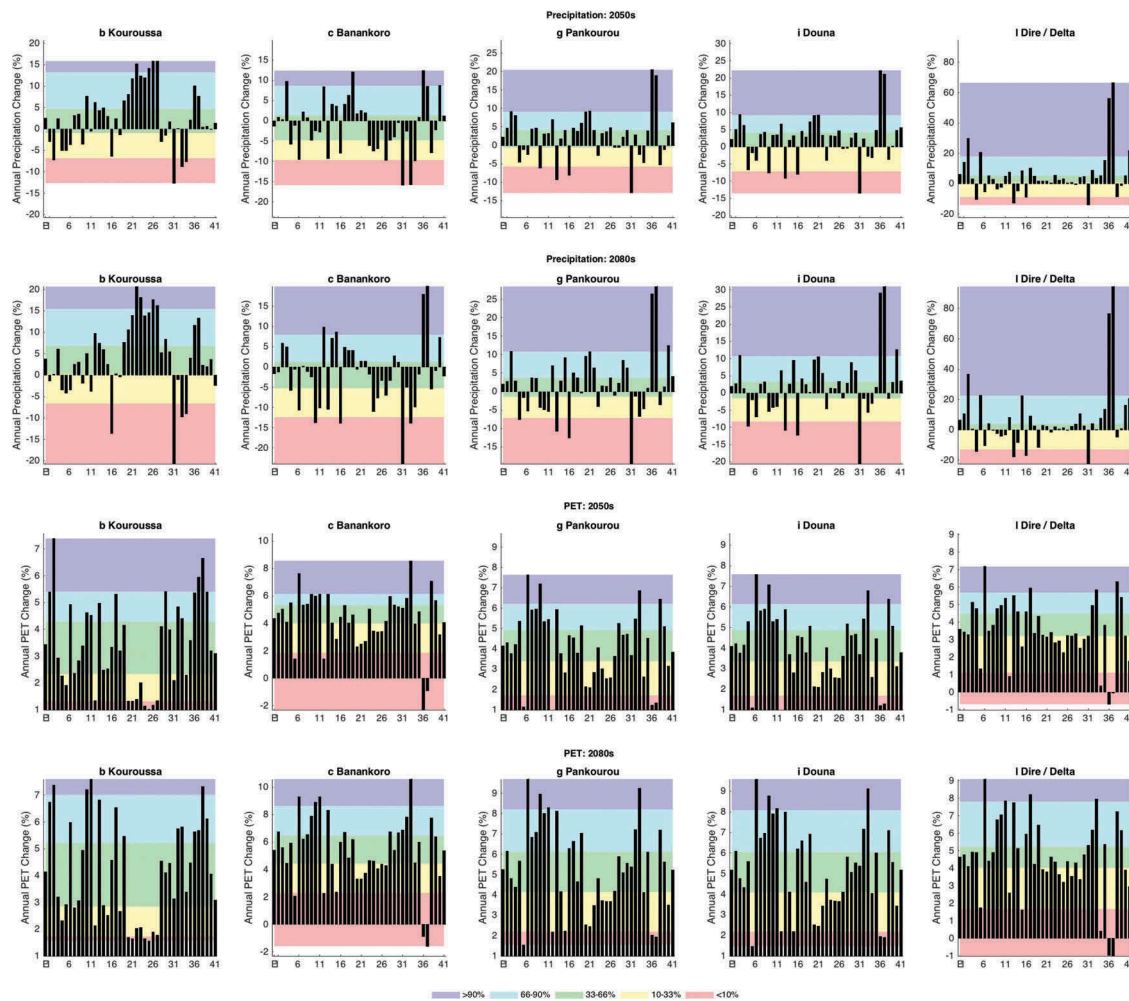


Figure 2. Percentage changes in mean annual precipitation and PET for five representative sub-catchments of the Upper Niger for each CMIP5 GCM and the ensemble mean for the 2050s and 2080s. Shaded bands represent the percentile ranges of the distribution of the CMIP5 ensemble. E: ensemble mean, 1–41: the CMIP5 GCMs shown in Table 1. (Note: y-axis ranges for precipitation and PET are consistent for individual sub-catchments for the two time slices but vary between sub-catchments.)

demonstrate that GCM-related uncertainty for scenario PET is considerably smaller than that for precipitation. For the 2050s the inter-GCM ranges of change in annual PET for the 10–90-percentile range vary between 3.8% (Sankarani – e) and 4.8% (Tinkisso – a). The mean range of 4.3% is over four times as small as the corresponding range for precipitation. For the 2080s the mean inter-GCM range is 5.8% (nearly a quarter of that for precipitation) and for individual sub-catchments varies between 4.5% (Kankan – d) and 6.4% (Bougouni – f). The central 33% of changes in annual PET (i.e. the 33–66-percentile range) has a mean of 1.4% (0.8–2.0%, Ke-Macina (j) and Kouroussa (b), respectively) for the 2050s and 1.9% (1.0–2.8%, Ke-Macina (l) and Tinkisso (a), respectively) for the 2080s. The 50-percentile changes for the 2050s are very similar throughout the Upper Niger, and range between 3.3% (Kouroussa – b) and 4.8% (Banankoro – c) with a mean of 4.2%. For the 2080s the 50-percentile changes are

slightly larger and again are similar throughout the catchment (mean: 5.2%, ranging from 4.1% (Kouroussa – b) to 5.8% (Tinkisso – a and Banankoro – c)). These figures are very similar (all within 0.6%) to those for the ensemble mean.

Scenario river flow

The impacts of the 41 CMIP5 GCMs upon mean, high and low flows for the 2050s and 2080s are summarized in Table 4. This shows simulated baseline mean, Q5 and Q95 discharges (discharges equalled or exceeded for 5 and 95% of the time, respectively) for the 12 gauging stations represented within the hydrological model. Percentage changes from the baseline for each of these discharges are provided for the ensemble mean, the two extreme changes projected by individual GCMs and a range of percentiles between 10 and 90%.

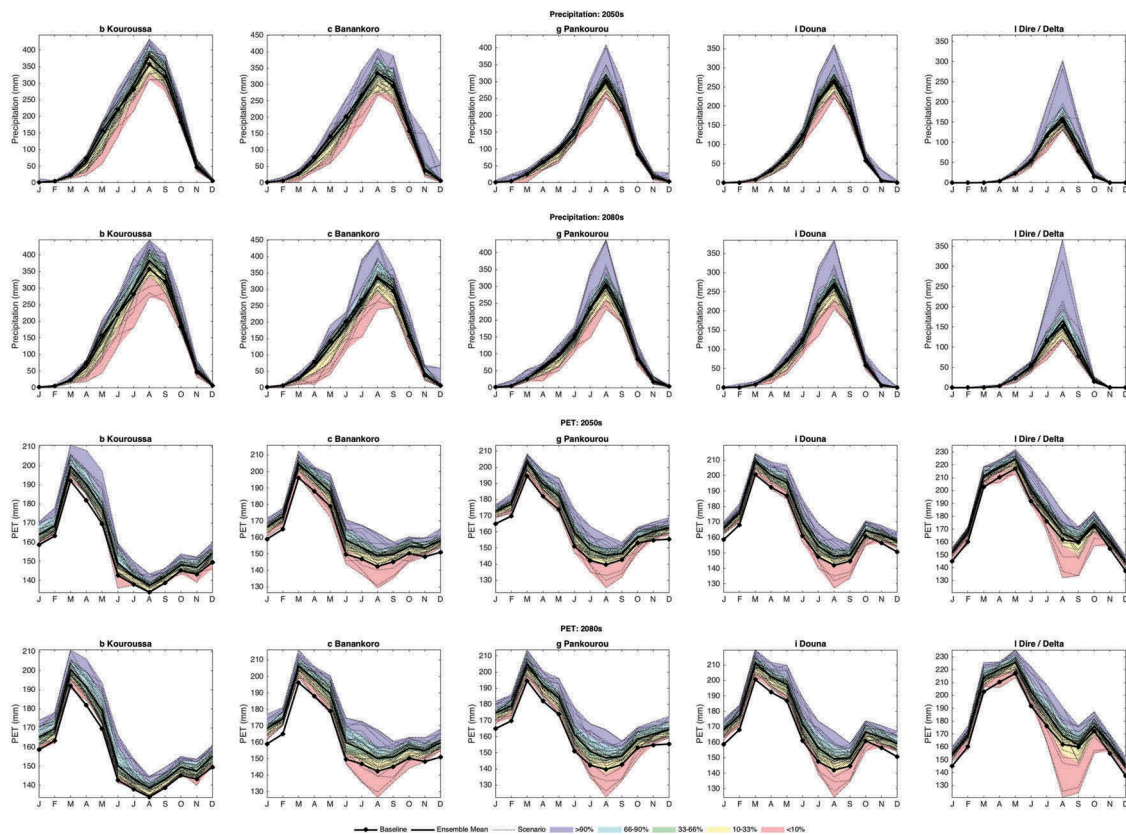


Figure 3. Mean monthly precipitation and PET for five representative sub-catchments of the Upper Niger for the baseline, each CMIP5 GCM and the ensemble mean for the 2050s and 2080s. Shaded bands represent the percentile ranges of the distribution of the CMIP5 ensemble. (Note: y-axis ranges for precipitation and PET are consistent for individual sub-catchments for the two time slices but vary between sub-catchments.)

The number (and percentage) of GCMs in which mean, Q5 and Q95 discharges increase are also shown. Figure 4 summarizes the impacts on mean discharges at six representative gauging stations in the form of percentage changes from the baseline for the ensemble mean and each GCM. These results are superimposed upon shaded bands representing the percentile ranges employed in Table 4. Changes in mean discharge are, at least in terms of direction of change, similar to those for Q5 and Q95 discharges. Impacts of each GCM and the ensemble mean upon the river regime (i.e. the mean monthly discharge) at the same six gauging stations are shown in Figure 5. These regimes, which are derived from the results for the 30-year simulation periods, are superimposed upon the same percentile range bands employed in Figure 4.

As for annual precipitation, both increases and decreases in mean, Q5 and Q95 discharges are projected for individual GCMs at all 12 gauging stations. There is a tendency for mean discharge to increase at slightly fewer gauging stations compared to the changes in mean annual precipitation over the 12 sub-catchments. The number of GCMs projecting

increases in mean discharge for the 2050s at individual stations varies between 16 and 25. For the 2080s mean discharge increases for between 12 and 25 GCMs. Out of the 492 gauging station–GCM combinations (i.e. 12 gauging stations \times 41 GCMs), mean discharge increases in 263 (53.5%) for the 2050s and 228 (46.3%) for the 2080s. The very large increases in annual precipitation for GCMs 36 and 37 over many sub-catchments are retained in the simulated mean discharges and river regimes (Figs 4 and 5, respectively). At the other extreme, GCM 31 is responsible for the largest decreases in mean, Q5 and Q95 discharges at all gauging stations.

The inter-GCM ranges of change in mean discharge vary considerably between gauging stations and for both the 2050s and 2080s are larger than those for mean precipitation. For example, beyond the most extreme changes (i.e. the 10–90-percentile range) the mean range of change in mean discharge for the 2050s is 52.9% (19.0% for precipitation) and varies between 31.0% (–20.7 to 10.3%, Dire – l) and 75.8% (–32.7 to 43.1%, Tinkisso – a). The corresponding mean for the 2080s is 59.5% (22.5% for precipitation) with a range of

Table 4. Baseline mean, Q5 and Q95 discharges ($m^3 s^{-1}$) and summary of changes (%) for the 41 CMIP5 GCM climate change scenarios for 12 gauging stations within the Upper Niger catchment. E.M. indicates the changes (%) for the ensemble mean, Max. and Min. represent the maximum and minimum changes (%), the corresponding figures for 90–10% represent the changes (%) for the respective percentile (which define the shaded zones in Fig. 4). Shaded cells indicate negative changes compared to the baseline. +ve and –ve are the number (%) of GCMs in which scenario mean discharges are above and below the baseline, respectively. Letters refer to the stations for the model sub-catchments indicated in Figure 1.

Parameter	Scenario	Gauging stations											
		a	b	c	d	e	f	g	h	i	j	k	l
Mean	Baseline	138.8	194.6	924.3	163.4	299.7	86.8	164.2	1235.2	340.9	1171.2	344.8	928.8
2050	E.M.	-2.5	2.7	-2.7	4.0	3.0	-11.5	1.1	-1.2	-1.9	-1.3	-2.0	-0.6
	Max.	61.2	36.2	40.0	31.9	38.5	81.3	116.5	43.8	117.2	47.4	119.2	29.3
	90%	43.1	25.0	14.9	21.5	20.1	17.4	27.1	16.0	25.7	16.7	25.6	10.3
	66%	5.7	4.9	2.6	15.7	10.7	3.8	7.2	3.7	7.2	3.9	7.2	3.1
	50%	-3.7	2.4	-1.2	7.7	6.9	-8.3	4.0	1.8	2.1	1.6	2.3	0.9
	33%	-16.8	-3.3	-4.9	-5.4	-2.6	-17.5	-1.5	-4.0	-6.9	-4.0	-6.9	-2.5
	10%	-32.7	-16.4	-24.4	-17.7	-21.4	-48.3	-45.4	-24.4	-47.7	-25.6	-46.7	-20.7
	Min.	-69.6	-36.0	-47.1	-30.2	-33.9	-73.6	-63.5	-44.4	-68.6	-46.4	-67.1	-40.0
	+ve	18 (44)	24 (59)	19 (46)	25 (61)	24 (59)	16 (39)	24 (59)	23 (56)	22 (54)	23 (56)	22 (54)	23 (56)
	-ve	23 (56)	17 (4)	22 (54)	16 (39)	17 (41)	25 (61)	17 (41)	18 (44)	19 (46)	18 (44)	19 (46)	18 (44)
2080	E.M.	-1.7	4.6	-3.1	4.0	2.4	-14.3	-2.8	-1.7	-5.7	-1.8	-5.5	-1.1
	Max.	91.8	44.4	55.1	42.5	51.1	112.3	169.0	58.7	171.4	64.1	179.5	39.0
	90%	56.5	32.5	14.4	27.1	22.0	23.2	30.1	15.9	28.2	16.5	28.3	10.3
	66%	8.3	11.3	4.9	16.8	13.2	-4.7	3.0	6.7	0.9	6.7	1.0	3.6
	50%	-6.9	5.5	-1.1	6.4	4.8	-11.8	-2.3	-0.1	-3.5	0.0	-3.0	-0.2
	33%	-18.9	-4.7	-8.7	-5.4	-5.0	-23.2	-12.5	-8.2	-19.1	-8.6	-18.7	-4.8
	10%	-39.3	-14.9	-24.5	-19.0	-18.6	-53.8	-56.9	-22.3	-58.9	-23.3	-57.6	-20.2
	Min.	-89.4	-57.1	-68.1	-51.5	-53.8	-92.5	-82.4	-64.9	-87.1	-67.6	-85.8	-62.8
	+ve	17 (41)	25 (61)	20 (49)	24 (59)	23 (56)	12 (29)	17 (41)	20 (49)	15 (37)	20 (49)	15 (37)	20 (49)
	-ve	24 (59)	16 (49)	21 (51)	17 (41)	18 (44)	29 (71)	24 (59)	21 (51)	26 (63)	21 (51)	26 (63)	21 (51)
Q5	Baseline	593.9	712.5	3602.2	624.5	1160.2	416.9	919.2	4726.2	1730	4709.5	1742	2128.7
2050	E.M.	-3.0	4.8	-1.1	6.1	1.8	-4.5	0.6	0.4	0.5	-2.9	-0.3	-0.8
	Max.	41.6	24.0	29.7	27.7	27.4	58.9	82.1	36.5	83.2	35.5	85.6	11.3
	90%	29.5	18.2	11.0	15.9	20.3	16.7	18.7	13.1	19.8	9.9	18.3	3.4
	66%	3.4	6.5	2.7	13.4	8.7	6.0	5.4	6.0	8.8	2.5	8.6	1.2
	50%	-3.5	4.6	0.7	10.4	4.5	-1.3	2.5	2.2	4.0	-0.5	3.6	0.6
	33%	-14.6	-1.9	-4.0	-2.0	-2.8	-8.2	-3.4	-1.8	-5.8	-4.5	-4.8	-1.3
	10%	-28.0	-9.4	-19.2	-14.3	-20.3	-36.0	-35.7	-19.3	-38.9	-22.0	-37.3	-8.1
	Min.	-58.9	-24.5	-37.5	-23.0	-28.5	-57.5	-54.9	-35.8	-60.1	-39.5	-59.0	-15.1
	+ve	18 (44)	27 (66)	22 (54)	26 (63)	26 (65)	19 (46)	23 (56)	25 (63)	23 (58)	20 (49)	24 (59)	23 (56)
	-ve	23 (56)	14 (34)	19 (46)	15 (37)	14 (35)	22 (54)	18 (44)	15 (37)	17 (42)	21 (51)	17 (41)	18 (44)
2080	E.M.	-1.2	5.9	-1.3	5.7	1.0	-6.9	-1.8	-0.6	-3.3	-3.7	-2.6	-1.3
	Max.	65.2	32.2	40.9	29.6	37.0	84.4	113.8	47.4	120.5	47.3	121.3	15.0
	90%	41.2	23.7	12.3	21.1	21.7	18.2	21.4	12.9	19.8	10.0	21.1	3.7
	66%	3.4	9.5	4.6	12.9	7.9	0.8	2.5	6.0	2.4	3.1	2.6	0.8
	50%	-4.2	3.4	1.2	6.7	2.1	-6.1	-0.8	2.6	-2.1	-0.3	-2.5	-0.5
	33%	-14.4	-0.9	-6.0	-1.2	-4.5	-14.2	-8.7	-6.9	-12.6	-9.3	-12.4	-1.8
	10%	-30.4	-10.6	-17.8	-12.7	-17.4	-41.2	-48.5	-16.5	-49.6	-19.5	-48.0	-9.0
	Min.	-82.4	-47.5	-59.5	-42.4	-42.9	-90.0	-77.5	-56.0	-84.8	-57.1	-83.8	-26.5
	+ve	17 (41)	26 (63)	22 (54)	28 (68)	24 (59)	16 (39)	18 (44)	24 (59)	18 (44)	20 (49)	19 (46)	19 (46)
	-ve	24 (59)	15 (37)	19 (46)	13 (32)	17 (41)	25 (61)	23 (56)	17 (41)	23 (56)	21 (51)	22 (54)	22 (54)
Q95	Baseline	0.6	3.3	7.9	1.5	0.2	0.1	0.1	10.1	0.3	0.0	0.8	0.0
2050	E.M.	-16.7	0.0	3.8	0.0	0.0	-100.0	0.0	-5.9	0.0	†	0.0	†
	Max.	183.3	51.5	63.3	33.3	50.0	0.0	100.0	40.6	1766.7	†	837.5	†
	90%	116.7	43.9	41.1	23.3	0.0	0.0	0.0	34.2	433.3	†	237.5	†
	66%	0.0	6.1	10.1	13.3	0.0	0.0	0.0	-1.5	100.0	†	50.0	†
	50%	-16.7	-3.0	0.0	0.0	0.0	-100.0	0.0	-9.9	66.7	†	25.0	†
	33%	-33.3	-10.6	-3.8	-6.7	0.0	-100.0	0.0	-15.3	0.0	†	-12.5	†
	10%	-50.0	-21.2	-20.3	-16.7	-50.0	-100.0	-100.0	-30.7	-100.0	†	-75.0	†
	Min.	-83.3	-45.5	-45.6	-26.7	-50.0	-100.0	-100.0	-52.5	-100.0	†	-75.0	†
	+ve*	13 (32)	18 (44)	19 (46)	19 (46)	1 (2)	0 (0)	2 (5)	14 (34)	25 (61)	†	23 (56)	†
	-ve	23 (56)	22 (54)	20 (49)	16 (39)	11 (27)	23 (56)	12 (29)	27 (66)	10 (24)	†	14 (34)	†
2080	E.M.	-16.7	0.0	3.8	0.0	0.0	-100.0	-100.0	-5.0	0.0	†	-12.5	†
	Max.	333.3	75.8	75.9	46.7	50.0	100.0	300.0	58.4	2866.7	†	1225.0	†
	90%	150.0	51.5	50.0	26.7	0.0	0.0	0.0	36.6	483.3	†	250.0	†
	66%	16.7	10.6	15.2	13.3	0.0	-100.0	0.0	9.4	66.7	†	31.3	†
	50%	-16.7	3.0	6.3	6.7	0.0	-100.0	0.0	-5.0	0.0	†	0.0	†
	33%	-33.3	-10.6	-7.0	-6.7	0.0	-100.0	-100.0	-19.3	-50.0	†	-50.0	†
	10%	-53.3	-22.7	-21.5	-20.0	-50.0	-100.0	-100.0	-31.7	-100.0	†	-75.0	†
	Min.	-100.0	-66.7	-67.1	-53.3	-50.0	-100.0	-100.0	-71.3	-100.0	†	-75.0	†
	+ve*	16 (39)	23 (56)	22 (54)	21 (51)	2 (5)	2 (5)	2 (5)	17 (41)	18 (44)	†	19 (46)	†
	-ve	23 (56)	17 (41)	17 (41)	17 (41)	12 (29)	27 (66)	19 (46)	22 (54)	17 (41)	†	20 (49)	†

† Q95 for baseline and all GCMs = 0 $m^3 s^{-1}$; * +ve and –ve do not sum to 100% as some Q95 discharges are unchanged.

Downloaded by [UCL Library Services] at 01:43 14 November 2017

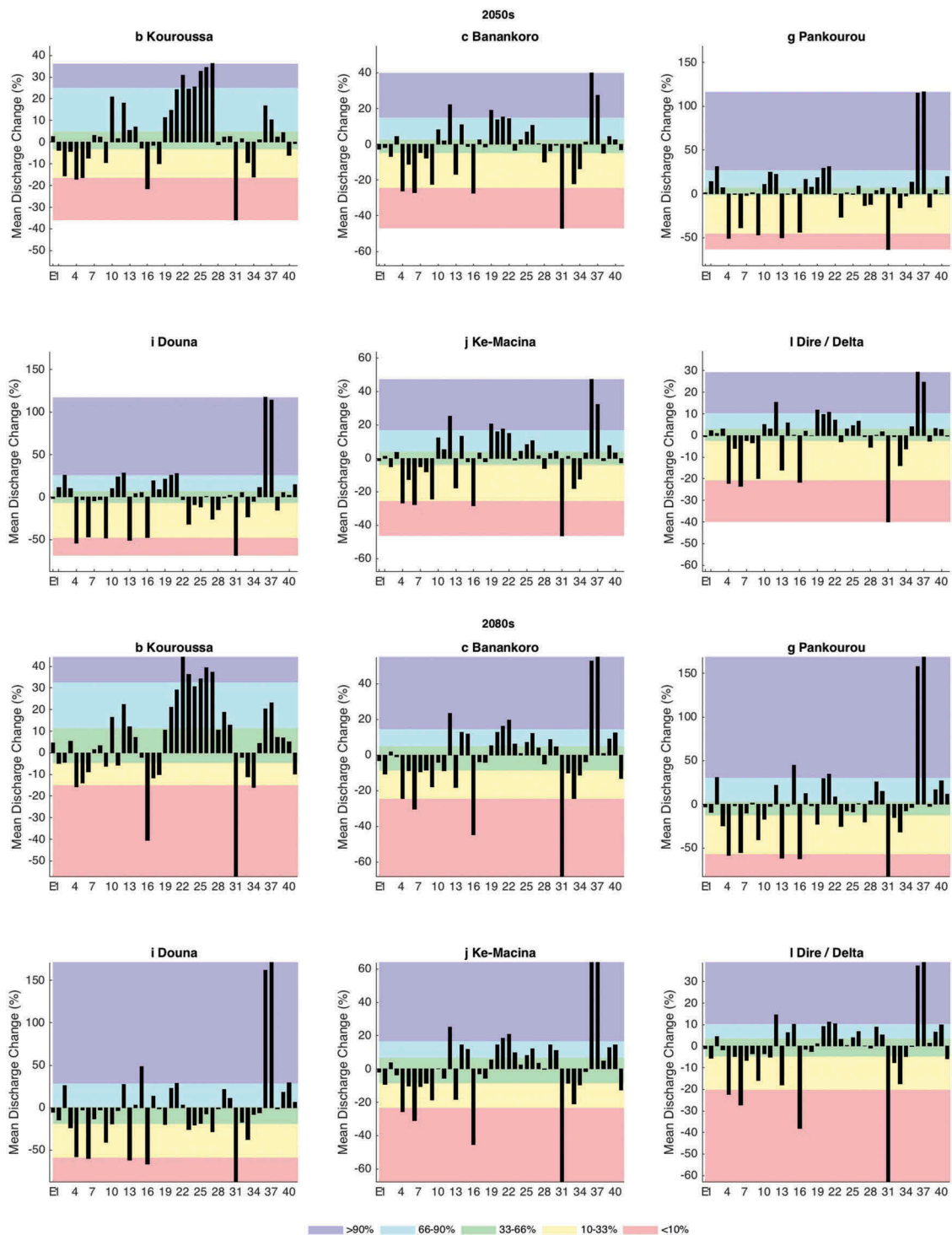


Figure 4. Percentage changes in mean discharges at six representative gauging stations in the Upper Niger for each CMIP5 GCM and the ensemble mean for the 2050s and 2080s. Shaded bands represent the percentile ranges of the distribution of the CMIP5 ensemble. E: ensemble mean, 1–41: the CMIP5 GCMs shown in Table 1. (Note: y-axis ranges are consistent for individual gauging stations for the two time slices but vary between gauging stations.)

between 30.5 and 95.8% (Dire: –20.2 to 10.3%, Tinkisso: –39.3 to 56.5%). The 10–90-percentile ranges of change in Q5 discharges are smaller than those for mean discharge (2050s mean: 40.3%, range: 11.4–58.5%; 2080s mean: 45.7%, range: 12.6–71.5%). Whilst

the inter-GCM ranges of change in low flows (Q95 discharges) are larger than those for mean discharge, absolute changes are small. The central 33% of changes in mean discharge (i.e. the 33–66-percentile range) are again predominantly larger than those for

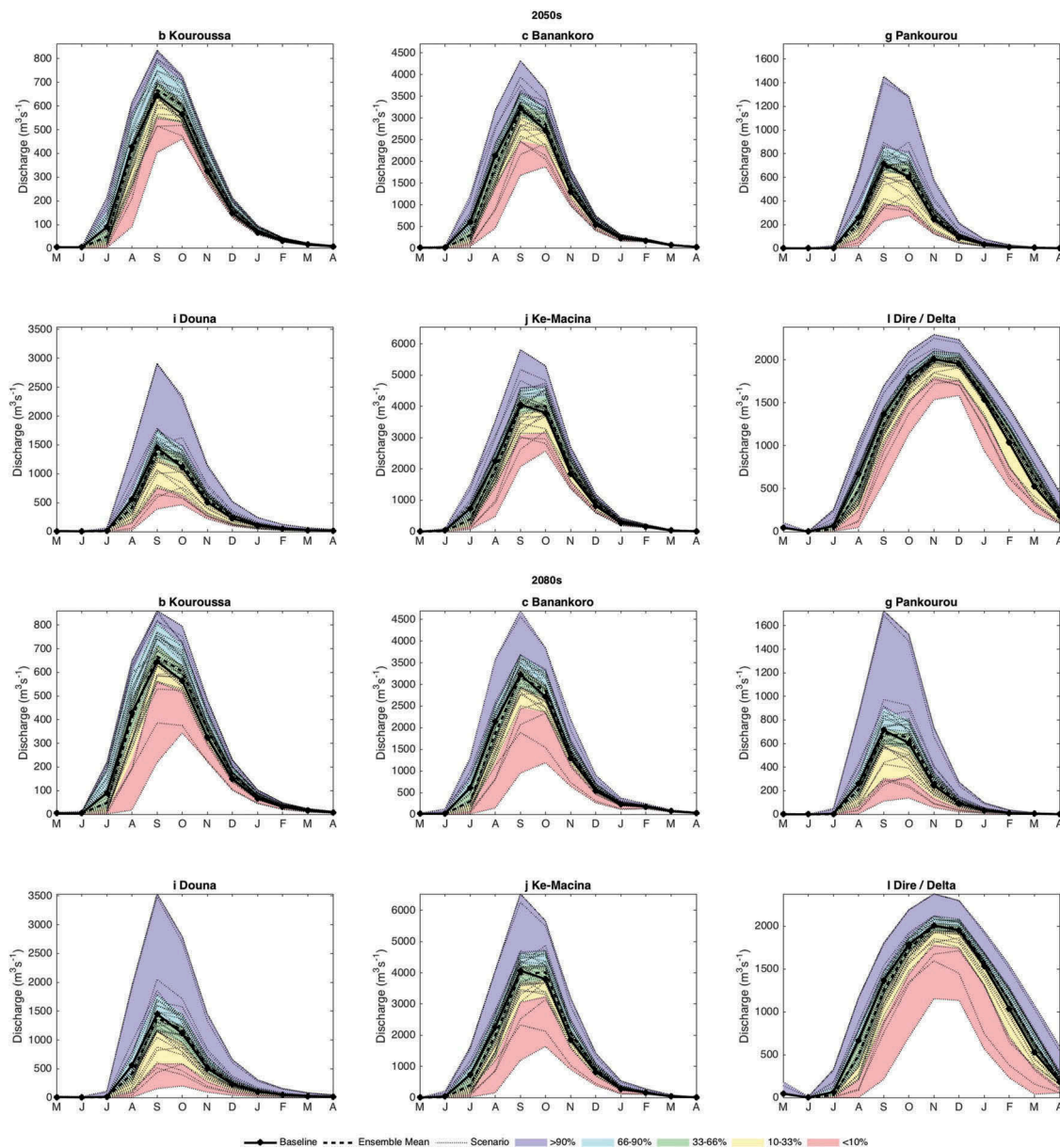


Figure 5. Simulated river regimes (mean monthly discharge) at six representative gauging stations in the Upper Niger for the baseline, each CMIP5 GCM and the ensemble mean for the 2050s and 2080s. Shaded bands represent the percentile ranges of the distribution of the CMIP5 ensemble. (Note: y-axis ranges are consistent for individual gauging stations for the two time slices but vary between gauging stations.)

precipitation. For the 2050s the mean range of change is 12.7% (5.6–22.6%) and for the 2080s it is 17.4% (8.4–27.2%). In both cases the extreme ranges of changes are associated with Dire – 1 and Tinkisso – a, respectively. Figure 5 shows that baseline river regimes are within or very close to the central 33% of scenario river regimes.

The 50-percentile changes in mean discharge for the 2050s, which are all relatively small, are positive at nine stations and negative at three (range: –8.3 to 7.7%, mean: 1.4%). This pattern is almost completely reversed for the 2080s, with positive changes at four stations and declines at eight (range: –11.8 to 6.4%,

mean: –1.0%). Peak (Q5) discharges follow a similar pattern, whilst slightly more 50-percentile Q95 discharges increase. Changes in mean discharge for the ensemble mean in both the 2050s and 2080s are positive at three gauging stations and decline at the remaining nine (Table 4), an almost perfect mirror of the changes in mean annual precipitation (Table 3). Changes are small in most cases, ranging between –11.5 and 4.0% (mean: –1.1%) for the 2050s and between –14.3 and 4.6% (mean: –2.2%) for the 2080s. Whilst in the 2050s an equal number of stations experience increases and decreases in Q5 discharges (range: –

4.5 to 6.1%, mean: 0.1%), in the 2080s declines in high flows are dominant, especially downstream (range: -6.9 to 5.9% , mean: -0.8%). Ensemble mean river regimes are very similar to the baseline (Fig. 5). Where declines in Q5 discharges are projected, the seasonal peak (September for stations above the Delta) tends to be lower than the baseline, although mean October discharges are higher at most stations. Q95 discharges both increase (2050s: six stations, 2080s: seven stations) and decrease.

Scenario impacts on the Inner Niger Delta

Figure 6 summarizes the impacts of the 41 CMIP5 GCMs on river inflows to the Inner Niger Delta. Using the approach adopted by Thompson *et al.* (2016), it shows the combined mean monthly inflows from Ke-Macina (j) and Beney-Kegny (k) for the baseline, each GCM and the ensemble mean for both the

2050s and 2080s. Percentage changes from the baseline in the annual total inflows are also shown for each GCM and the ensemble mean for both time slices. Both the monthly inflows and the changes in the annual total inflows are superimposed on the same percentile ranges used in the previous analyses.

For the 2050s increases in the mean annual inflow to the Inner Niger Delta are projected by 25 (61%) of the 41 GCMs, with the remaining 16 (39%) projecting declines. In the 2080s more GCMs (23/56%) project reductions than those that project increases (18/43%). The largest reductions are associated with GCM 31, whilst GCMs 36 and 37 dominate the largest increases. The 10–90-percentile range of change in annual river inflows is very similar for the 2050s and 2080s at 49.3% (-29.4 to 19.9%) and 48.2% (-27.9 to 20.3%), respectively. The central 33–66-percentile range is, however, slightly larger in the 2080s (13.1% ; -7.9 to 5.2%) compared to the 2050s (9.6% ; -4.4 to 5.2%). Whilst baseline

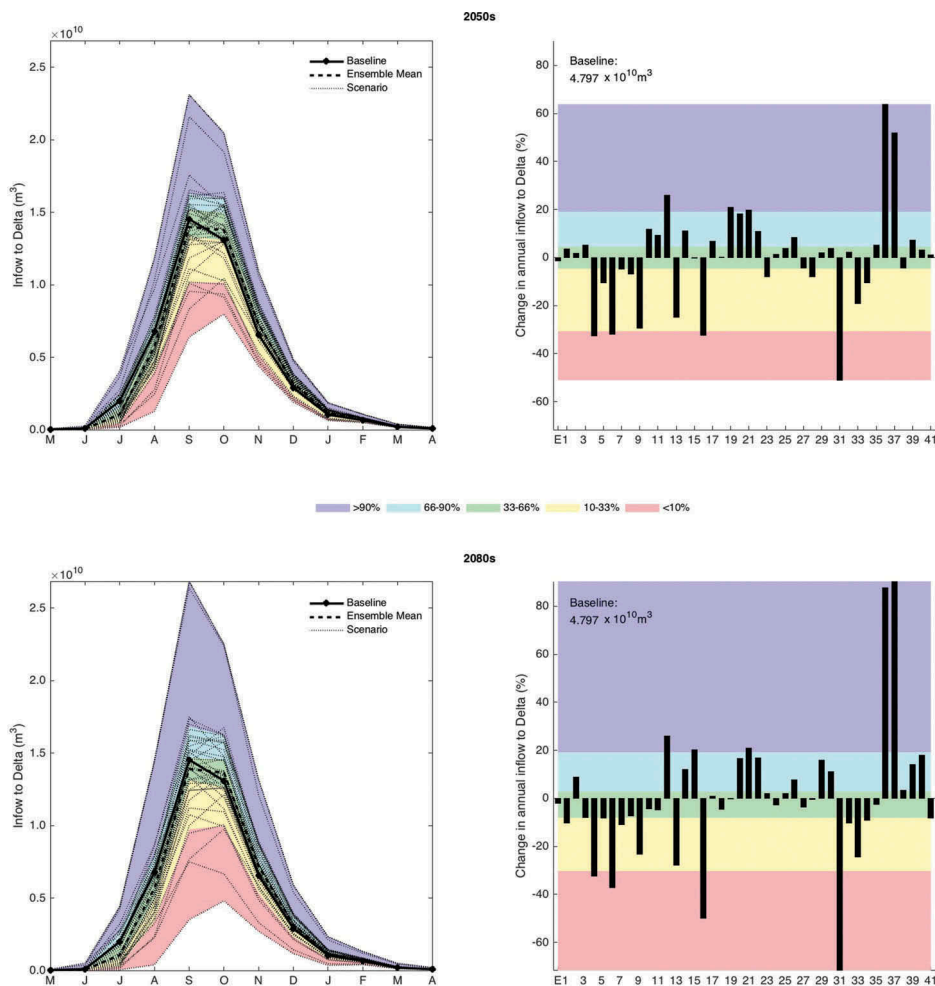


Figure 6. Simulated mean monthly river inflows to the Inner Niger Delta for the baseline, each CMIP5 GCM and the ensemble mean for the 2050s and 2080s; changes from the baseline in mean annual inflows for each CMIP5 GCM and the ensemble mean for the 2050s and 2080s. Shaded bands represent the percentile ranges of the distribution of the CMIP5 ensemble. E: ensemble mean, 1–41: the CMIP5 GCMs shown in Table 1.

mean monthly inflows fall within the central 33% of changes in both time slices during the peak flow period (September and October), they are just above it during the rising limb of the annual flood, with these increases being compensated by declines during the subsequent recession (Fig. 6). The 50-percentile change in annual inflows for the 2050s is very slightly positive (2.1%), whilst a decline of a similar magnitude (−2.5%) is projected for the 2080s. The ensemble mean for both time slices results in small reductions in mean annual inflows of −1.4 and −2.1%, respectively. Mean monthly inflows for the ensemble mean for both the 2050s and 2080s are very similar to the baseline (Fig. 6). In both time slices, peak September flows decline slightly (by 3.7 and 4.3% respectively) but are still larger than those in October, which increase slightly (by 5.2 and 4.3%, respectively) compared to the baseline.

Figure 7 shows mean monthly flood extent within the Inner Niger Delta for the baseline, each of the 41 CMIP5 GCMs and the ensemble mean for both the 2050s and 2080s. Model results are superimposed upon the percentile range bands employed in previous analyses. The wide range in flood regimes projected by the different GCMs is clearly demonstrated. In most cases and both time slices the baseline November peak is retained. For the 2050s only one GCM (GCM 16) projects a mean seasonal peak in another month (October), whilst in the 2080s three GCMs (GCMs 3, 13 and 16) suggest a mean seasonal peak that occurs 1 month earlier. A larger number of GCMs project declines in the seasonal peak flood extent compared to those that project increases. Of the 41 GCMs, 32 project declines in both October and November mean flood extent for the 2050s. Three of the remaining nine GCMs project declines in October, so that only six project enhanced flooding in the two peak inundation

months. For the 2080s, 28 of the GCMs project declines in flooding for both October and November, with a further four projecting declines in October alone. Increased inundation in both peak months is projected by nine GCMs. The apparent anomaly between changes in annual river inflow to the Inner Niger Delta (increases for 25 and 18 of the 41 GCMs for the 2050s and 2080s, respectively) and peak flood extent is explained by projected climate changes over this part of the basin. Whilst more GCMs project increases rather than decreases in annual precipitation over the Dire/Delta sub-catchment (I), baseline precipitation is low. In contrast, this part of the basin has the highest baseline annual PET and, with the exception of two GCMs, it is projected to increase (Table 3 and Fig. 2). As a result, net precipitation (precipitation – PET) only increases for seven GCMs in both time slices. In many cases, enhanced evaporation from the inundated area counteracts the influence of increased river inflows when they occur.

Impacts of these changes are evident in the relative position of the baseline flood regime and the central 33–66-percentile range of change in mean monthly flood extent (Fig. 7). In the 2050s this central range is below the baseline between August and November, and the baseline flood regime is instead located within the 66–90-percentile range. The period when the baseline regime is within this higher range extends into December for the 2080s. During the latter part of the flood recession between January (December for the 2050s) and March, as well as at the start of the annual rise in water levels (July), the baseline regime falls within the 33–66-percentile range of change. Conversely during the low water period, the baseline lies within the 10–33-percentile range since a majority of GCMs project increased flooding. For the 2050s,

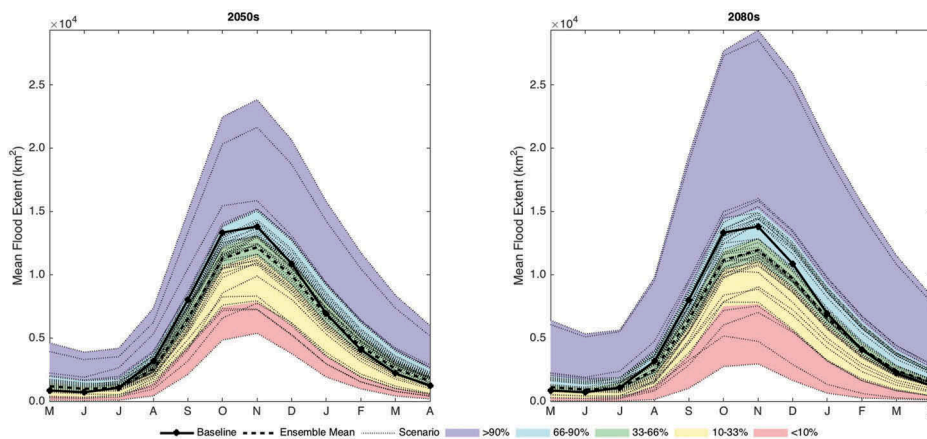


Figure 7. Mean monthly flood extents for the Inner Niger Delta for the baseline, each CMIP5 GCM and the ensemble mean for the 2050s and 2080s. Shaded bands represent the percentile ranges of the distribution of the CMIP5 ensemble.

flood extent between April and June is above the baseline for 33 of the 41 GCMs. This declines to 31 for the 2080s. The ensemble mean reflects the dominance of declines in peak flood extents and increases in dry season flooding. For both the 2050s and 2080s, the mean monthly flood extent for this scenario is below the baseline between July and January, with peak (October and November) areas of inundation declining by on average 1841 km² (13.6%) in the 2050s and 2024 km² (14.9%) in the 2080s. Conversely, mean monthly flood extents are very slightly above the baseline between February and June.

Figure 8 summarizes the climate change impacts on annual maximum flood extents. For both the 2050s and 2080s it plots peak seasonal flood extent against the numbers of years in which they are equalled or exceeded during the 30-year simulation periods. This is done for the baseline, each GCM and the ensemble mean. Change from the baseline for the largest, mean and smallest annual peak flood extents are also shown. Changes in mean annual maxima are close to those of November within the flood regime (Fig. 7); small differences are due to changes in timing of the annual peak. As in previous analyses, results are superimposed upon

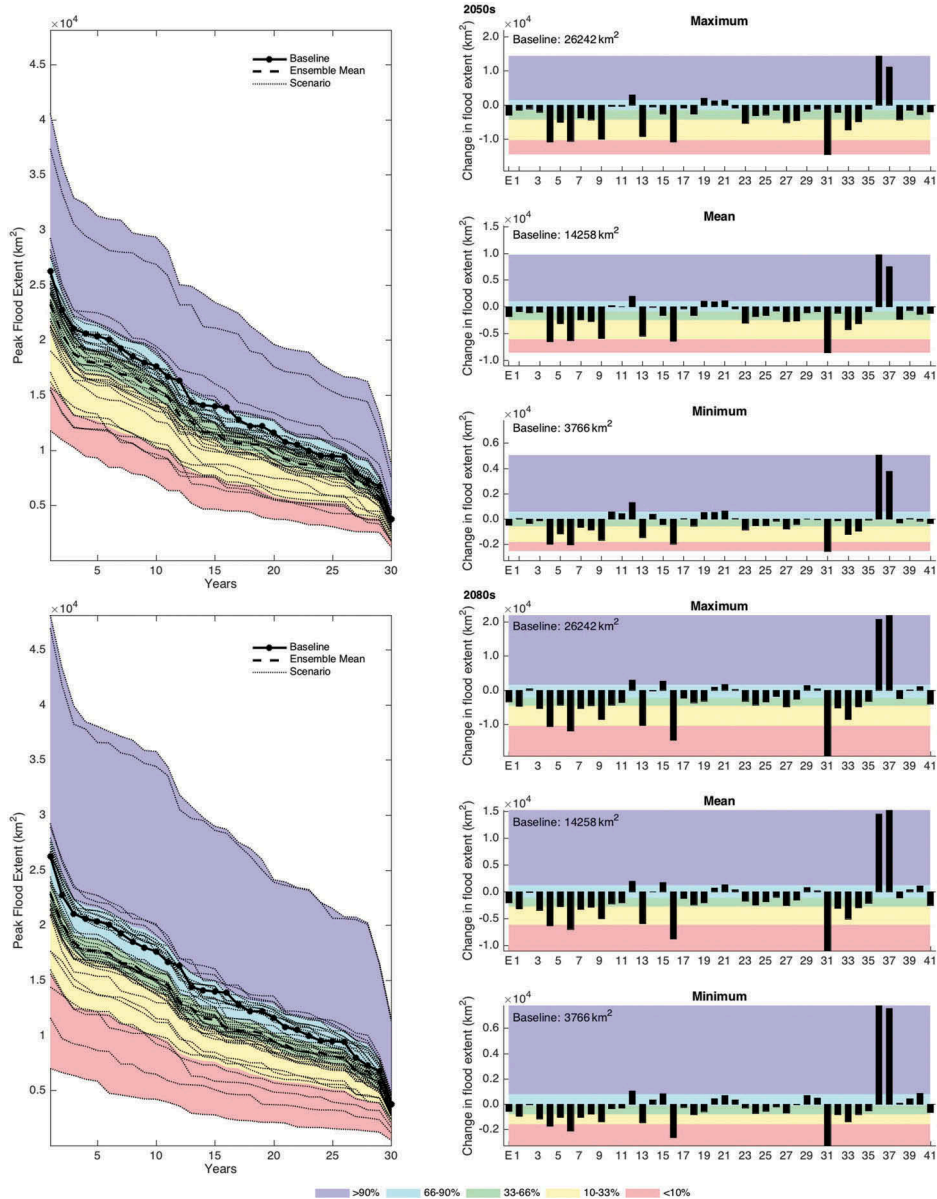


Figure 8. Impacts of climate change on annual peak flood extents within the Inner Niger Delta for the 2050s and 2080s: peak flood extent–frequency for the baseline, each CMIP5 GCM and the ensemble mean; change from the baseline in the maximum, mean and minimum annual peak flood extents for each CMIP5 GCM and the ensemble mean. Shaded bands represent the percentile ranges of the distribution of the CMIP5 ensemble. E: ensemble mean, 1–41: the CMIP5 GCMs shown in Table 1.

percentile range bands. The dominant trend of declines in peak flood extent is clearly evident. For the 2050s, 22 GCMs project declines in all 30 annual peak flood extents. A further four project declines in all but one year. In contrast, only three GCMs show consistent increases for the full 30 years. Unsurprisingly these include GCMs 36 and 37 (the other being GCM 12). Only one GCM projects increases in all but one year, whilst two further GCMs project declines in all but two years. Mean peak flood extent declines for 33 GCMs, with only eight projecting increases. Excluding the more extreme changes produces a 10–90-percentile range for the 2050s of -6136 km^2 (-43.0%) to 987 km^2 (6.9%), whilst the boundaries of the central 33% of changes (33–66-percentile range) are both negative, ranging between -2534 km^2 (17.8%) and -931 km^2 (-6.5%). The ensemble mean produces a reduction in annual peak flood extent of 1870 km^2 (13.1%). Very similar trends are evident in the smallest and largest annual floods (Fig. 8). In percentage terms, changes in the smallest flood extents tend to be greater than those for the mean, although absolute changes are obviously smaller. Conversely, percentage changes in the largest floods tend to be smaller than the mean (absolute changes being larger).

A similar picture emerges for the 2080s although, as with projected meteorological and river discharge changes, the inter-GCM range expands from the 2050s (Fig. 8). Declines still dominate, with 26 GCMs projecting reductions in peak flood extent throughout the 30 years, whilst two project declines in 28 years (none projecting declines in 29 years). Five GCMs project increases in peak flood extent in all 30 years, with one and two projecting increases in 29 and 28 years, respectively. The number of GCMs projecting lower mean peak flood extent reduces to 30 (11 projecting increases). Changes for the 10–90-percentile range vary between -6176 km^2 (-43.3%) and 1165 km^2 (8.2%), whilst the central 33–66-percentile ranges from -2835 km^2 (-19.9%) to -1228 km^2 (8.6%). A reduction in mean peak annual flood extent of 2076 km^2 (14.6%) is projected for the ensemble mean. Reductions in the smallest and largest annual floods are projected by 28 and 29 GCMs, respectively (Fig. 8). For both the smallest and largest peak annual flood extents, the central 33–66-percentile ranges of change are bounded by declining flood extent, whilst the ensemble mean is associated with declines of 561 km^2 (14.9%) and 3351 km^2 (12.8%), respectively.

Implications on climate change projections of the genealogy-based GCM groups

Figure 9 summarizes the impacts of the climate change scenarios for the 12 GCM groups that were established

using GCM genealogy. For illustrative purposes it shows changes from the baseline in mean annual precipitation and PET as well as mean discharge for three of the sub-catchments/gauging stations for which comparable results were shown in Figures 2 and 4, respectively. These were selected to represent the upstream/western, middle/central and downstream/eastern parts of the Upper Niger. For both the 2050s and 2080s results are shown for the original ensemble mean scenario based on all 41 GCMs, the group ensemble mean derived from the 12 GCM groups and each of the individual groups. Simulated river inflows to the Inner Niger Delta (comparable to Fig. 6) as well as the mean monthly flood extent and change in mean peak flood extent (comparable to Figs 7 and 8, respectively) are also shown for these scenarios.

Whilst there are some subtle differences between results for the genealogy-based GCM groups and the complete 41 GCM ensemble, the main trends previously described for the latter are retained. In all sub-catchments different GCM groups project increases and decreases in annual precipitation (Fig. 9). Increases are projected in 71 (49.3%) and 75 (52.1%) of the 144 sub-catchment–GCM group combinations (12 sub-catchments \times 12 GCM groups) in the 2050s and 2080s, respectively (close to the 56.1 and 52.6% for the 41 GCM ensemble). Across the 12 sub-catchments changes in annual mean precipitation for the group ensemble mean are small, varying between -3.2 and 3.6% (2050s) and -3.4 and 4.6% (2080s). There are fewer positive changes compared to the original ensemble mean (three compared to eight for the 2050s, seven compared to nine for the 2080s), although differences between the two are small (mean differences: -1.9 and -1.7% for the two time slices, respectively). Differences between the original and group ensemble means are very small (all $<0.2\%$) for annual PET. Small ($<5\%$) declines for Group 9 are only projected in two sub-catchments (Kankan – d and Sankarani – e; not shown) with the relatively large increases in PET projected by GCM 35 (Fig. 2) cancelling out those previously described for the other two GCMs in this group (GCMs 36 and 37). Annual PET increases for all the other scenarios, although the inter-GCM group range is, as for the full 41 ensemble, much smaller than that of precipitation (by around five times in percentage terms for both time slices).

As for the 41 GCM ensemble, increases and decreases in mean discharge are projected by different GCM groups (Fig. 9). In both time slices 66 (45.8%) of the 144 gauging station–GCM group combinations project increases (compared to 53.5% (2050s) and 46.3% (2080s) for the 41 GCMs). Also in common with the 41 GCM ensemble, the mean inter-GCM

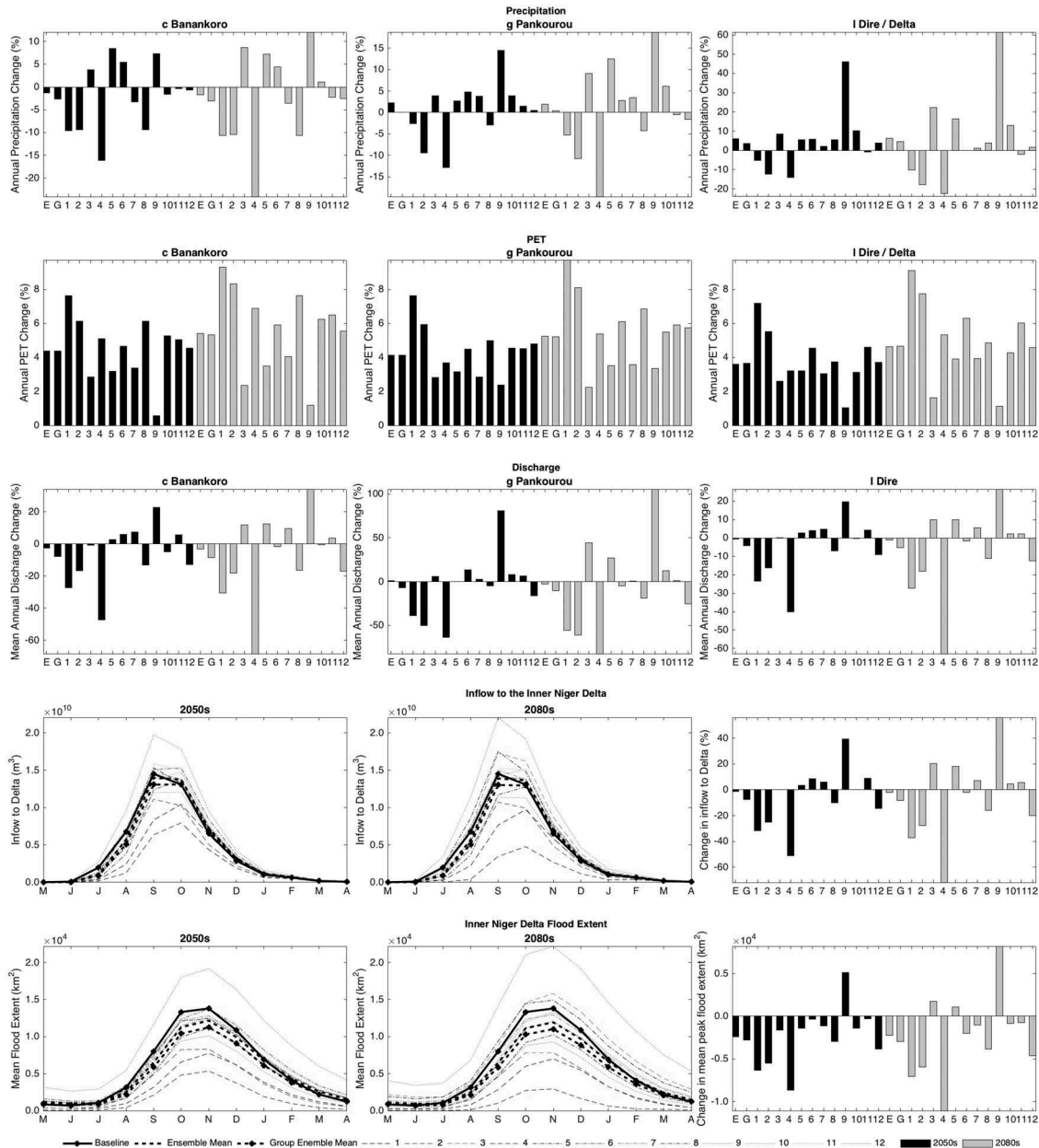


Figure 9. Summary of the impacts of GCM group scenarios on the Upper Niger and Inner Niger Delta: percentage change in mean annual precipitation and PET for three representative sub-catchments; change in mean discharge at three representative gauging stations; mean monthly river inflows to the Inner Niger Delta and percentage changes in mean annual inflows; mean monthly flood extent and changes in mean peak flood extent within the Inner Niger Delta. E: ensemble mean of the 41 CMIP5 GCMs, G: group ensemble mean of the 12 GCM groups, 1–12: the GCM groups shown in Table 2. (Note: y-axis ranges vary between sub-catchments/gauging stations.)

group range of change in mean discharge is, in percentage terms, around three times as large as that of mean annual precipitation. Unlike the original ensemble mean, the group ensemble mean is associated with declines in mean discharge at all 12 gauging stations in both time slices. On average, mean discharge for the latter scenario declines by 7.3% (2050s) and 8.7% (2080s) compared to the declines of 1.1 and 2.2% for the original ensemble mean.

The declines in mean annual river inflow to the Inner Niger Delta for the group ensemble mean (2050s: -7.5% , 2080s: -8.2%) are around 6% larger than those of the 41 GCM ensemble mean. Inflows increase for seven (2050s) and six (2080s) of the GCM groups, declining for the others. Although the largest declines are identical to those of the 41 ensemble since they are associated with Group 4, which comprises only one GCM (INM-CM4), the largest increases are reduced as a result of grouping

the three MIROC GCMs (Group 9). This is repeated for the changes in mean peak flood extent (Fig. 9). Of the 12 GCM groups, increases are only projected by one in the 2050s, increasing to three for the 2080s. In both time slices the declines in mean peak inundation projected by the group ensemble mean are around 6% larger than those of the 41 GCM ensemble mean (2050s: $-2777 \text{ km}^2/19.5\%$, 2080s: $-2977 \text{ km}^2/20.9\%$).

Discussion

There are consistencies between the climate results from the current study and those of the earlier investigation by Thompson *et al.* (2016), which employed the same hydrological model and a smaller set of projections from seven GCMs for a consistent 2°C increase in global mean temperature. The addition of more GCMs compared to the earlier study increases the range of inter-GCM uncertainties in projected changes in hydro-meteorological conditions in the Upper Niger. Both studies demonstrate much larger inter-GCM uncertainty in precipitation compared to PET. Whilst the vast majority (all in the case of the earlier study) of sub-catchment–GCM combinations are associated with increases in PET, both increases and decreases in mean annual precipitation are projected by different GCMs in both studies. Similarly, the much larger percentage ranges of change in annual precipitation for the current study (Fig. 2, Fig. 9 for the GCM groups) echo those of Thompson *et al.* (2016), in which the mean range of change in annual precipitation exceeded that of PET by over five times (compared to around four times in the current study for the full 41 GCM ensemble and five times for the genealogically-based GCM groups). Larger uncertainty in precipitation, including variations in the direction of change, compared to PET reflects results from other studies (Kingston and Taylor 2010, Kingston *et al.* 2011, Singh *et al.* 2011, Thompson 2012, Thompson *et al.* 2013). For example, Ho *et al.* (2016) used the same approach and GCMs as those employed in the current study in their assessment of climate change impacts on river flow within Brazil's Tocantins–Araguaia Basin. For a 2080s time slice, changes in mean annual precipitation varied between -25.1 and $+21.8\%$ (total range 46.9%) compared to increases in PET of between 1.9 and 13.9% (range 12% , nearly a quarter of the range for precipitation).

Elevated evapotranspiration results in slightly more GCMs projecting declines in discharge compared to precipitation, although considerable uncertainty in the direction of change remains (Figs 4 and 5, Fig. 9 for the GCM groups). In common with an earlier study using a single GCM and hydrological models of four West

African catchments (Ardoin-Bardin *et al.* 2009), changes in river flow tend to follow projected changes in precipitation. Whilst inter-GCM patterns of changes in mean discharge at gauging stations in upstream sub-catchments closely correspond with those for mean annual precipitation over their sub-catchments (e.g. Koroussa (c) and Pankourou (g) in Figs 2 and 4), further downstream, and as reported by Thompson *et al.* (2016), the cumulative influence of changes in climate and, in turn, runoff over different sub-catchments impact the degree of direct correspondence. Similar results were identified by Thompson *et al.* (2013, 2014a) for the Mekong River Basin, where variations in climate change responses between different downstream sub-catchments either amplified or diminished projected changes in runoff from further upstream. The larger inter-GCM ranges of change in discharge compared to precipitation (by two–three times for the 10–90-percentile range) replicates results reported by Thompson *et al.* (2016) for the smaller set of GCMs over the Upper Niger. They also reflect the larger observed declines since the 1970s in discharge of the Bani compared to precipitation (-69% versus -15 to -25% ; Louvet *et al.* 2011). Elsewhere, Ho *et al.* (2016) showed that the inter-GCM range of change in discharge for the Tocantins–Araguaia Basin and the same GCMs as those employed in the current study was 2.2 times the magnitude of the range for precipitation.

Uncertainties in the direction of change in river inflows to the Inner Niger Delta from the current study (Fig. 6) contrast with the results of Thompson *et al.* (2016), who found that, of the smaller set of seven GCMs, only one projected modest (3.9%) increases in annual inflow to the Inner Delta. Of the remaining six GCMs, three projected declines in inflows of less than 5% , with results for the remaining three suggesting declines of between 18.1 and 52.7% . These are of a comparable magnitude to the changes projected by some GCMs in the current study.

Whilst there is some uncertainty in the direction of change in flood extent within the Inner Niger Delta (Figs 7–9 for the GCM groups), the relative dominance of declines in annual peaks echoes those reported by Thompson *et al.* (2016) where only one out of seven GCMs projected increases in mean peak flood extent (of 1405 km^2). This one change is of a similar magnitude to those resulting from a number of the GCMs in the current study, although it is considerably lower than the largest changes simulated by GCMs 36 and 37. Of those GCMs projecting declines in mean flood extent in the current study, the magnitude of change in at least one (two for the 2080s) exceeds the largest decline reported by Thompson *et al.* (2016) of

7903 km². Many of the declines reported herein are larger than those projected by the remaining five GCMs in the earlier study. Model results illustrate the impact of drier local conditions projected by most GCMs. These result from increases in evapotranspiration over the part of the basin that has the highest baseline annual PET and lowest annual precipitation. Evapotranspiration can be a major term in the water balance of many wetlands (e.g. Gasca-Tucker *et al.* 2007, Baker *et al.* 2009) and evaporation losses can increase substantially during periods of inundation within floodplains (e.g. Clilverd *et al.* 2016). Mahé *et al.* (2009), for example, demonstrated increases in these losses from the Inner Niger Delta as flood extent increased. This process is particularly important within many of Africa's major floodplains, including the Inner Niger Delta, which are located in relatively dry areas compared to the uplands from where their river inflows are derived (e.g. Sutcliffe and Parks 1989, Thompson 1996). Under these conditions, the model simulates increases in evaporation losses from the inundated area that are relatively infrequently offset by higher local precipitation. Only GCMs that project the very largest increases in river inflow lead to larger simulated flood extents and, as a consequence, the dominant, but by no means exclusive, trend is for declines in seasonal inundation.

Whilst the ensemble mean from a relatively large number of GCMs should serve as a better indicator of climate change impacts than the results of a single GCM, it does, as discussed above, rely on GCM independence (Pirtle *et al.* 2010). The potential influence upon climate change projections of using a number of GCMs from the same institution or GCMs with shared model code was addressed in the current study by grouping GCMs according to their genealogy. Although results for the ensemble mean scenario developed from the resulting 12 GCM groups tend to be associated with slightly drier conditions than those derived from the mean of the 41 GCM ensemble, differences are generally small, echoing the results of Ho *et al.* (2016), who used the same approach to grouping GCMs. On average across the 12 sub-catchments the ensemble mean for the 41 GCMs results in small increases in mean annual precipitation (average increases of 1.1 and 1.3% for the 2050s and 2080s, respectively), although both relatively small decreases and increases (−2.0 to 6.5%) are projected for individual sub-catchments. These inter-sub-catchment variations in the direction of change are repeated for the group ensemble mean, although the average change is negative (−0.8 and −0.4% for the two time slices, respectively). PET increases throughout the basin for

both ensemble means (in both cases by on average 4.0 and 5.0%, for the 2050s and 2080s, respectively). Whilst most, but not all, gauging stations experience declines in mean discharge for the 41 GCM ensemble mean scenario, the group ensemble mean leads to catchment-wide declines. The magnitudes of these changes are small (on average 1.1 and 2.2% for the two time slices, respectively, in the case of the 41 GCM ensemble mean, with those of the group ensemble mean declining by a further 6%). For the reasons discussed above, larger reductions in the annual peak flood extent (13.1 and 14.6% in the 2050s and 2080s, respectively) are projected for the 41 GCM ensemble mean. These reductions increase in magnitude to 19.5 and 20.9% for the group ensemble mean.

Given variable biases of individual GCMs in reproducing observed climate (Tebaldi and Knutti 2007), GCM-related uncertainty in projected changes in climate, river flow and flooding for the Upper Niger could be further constrained using GCM reliability ratings derived through the comparison of observed and simulated climate over the region (e.g. Maxino *et al.* 2008, Perkins *et al.* 2007; Ghosh and Mujumdar 2009). In this way, GCM projections could be weighted according to their ability to reproduce regional climate. Climate change assessments for the Upper Niger could also be extended through consideration of the more extreme RCP scenarios (2.6 and 6.0/8.5; Moss *et al.* 2010, van Vuuren *et al.* 2011) with a view to assessing hydro-climatological responses to alternative emissions scenarios and their impacts on GCM-related uncertainty (e.g. Gosling *et al.* 2011, Thompson *et al.* 2013). A number of previous studies (Hirabayashi *et al.* 2013, Koirala *et al.* 2014) have, for example, shown greater agreement in the direction of change in river flows projected by atmosphere–ocean general circulation models when considering the most extreme RCP8.5 scenario compared to the intermediary RCP4.5 scenario used herein. Repeating our analysis using the RCP8.5 scenario would permit an assessment of whether the stronger model agreement revealed by these global-scale analyses is repeated at the scale of the Upper Niger and the Inner Niger Delta.

The variable changes in river flow of the Upper Niger and flood extent within the Inner Niger Delta that are projected by different GCMs will clearly have very different environmental and water resource implications. A river's flow regime exerts a dominant influence upon ecological processes, biodiversity and ecosystem integrity (e.g. Poff *et al.* 1997). Equally, the dominant influence of a wetland's hydrological regime, including the magnitude and variability in flood extent, upon ecosystem functioning and, in turn, ecosystem

service delivery is widely acknowledged (Baker *et al.* 2009, Maltby *et al.* 2011). For example, in Africa's floodplain wetlands, including the Inner Niger Delta, the annual flood is particularly significant in sustaining fisheries, providing wildlife habitat, including for waterbirds, as well as underpinning the human utilization of the wetland for agricultural productivity such as rice cultivation (e.g. Adams 1992, Polet and Thompson 1996, Thompson *et al.* 2016). Changes in flood patterns within the Inner Delta over recent decades have already impacted rice cultivation, fishing and grazing (Goosen and Kone 2005, Zwarts and Diallo 2005, Zwarts and Kone 2005b). Declines in flood extent projected by many of the GCMs in the current study are likely to reduce these ecosystem services, which could, given the large human population that is reliant upon them, have significant socio-economic consequences. Conflicts are more likely between human uses of water resources and the water requirements of ecosystems such as the floodplain wetlands, which could, in turn, have implications for globally significant wildlife populations. Alternatively, the increases in discharge and enhanced flooding projected by some GCMs could maintain aquatic ecosystems, benefit fisheries via the expansion of floodplain nurseries (e.g. Welcomme 1986, Nestler *et al.* 2012) and support extension of some human activities, such as floodplain agriculture. It is, however, possible that increased flooding, especially during periods of normally relatively low water levels, could have detrimental ecological implications. For example, increases in dry season river flows and/or flooding within wetlands in Africa (e.g. Goes 2002, Blaser 2013) and elsewhere (e.g. Meynell *et al.* 2012) have facilitated changes in vegetation, including the expansion of invasive species, with implication for access to wetland resources by people and wildlife.

As acknowledged by Thompson *et al.* (2016), detailed evaluation of the ecological impacts of projected hydrological changes would be a major undertaking, especially given the lack of detailed knowledge of hydro-ecological relationships that are likely to vary in space and time over such a large geographical area as the Upper Niger. In response to the growing recognition of the need to sustain “environmental flows”, a term widely used to describe the flow regime of a river that is required to maintain economically, socially and ecologically important ecosystem services (e.g. Dyson *et al.* 2003), a range of methods for assessing potential impacts of hydrological change have been developed. These acknowledge the influence of different components of the regime that can be described by variability, magnitude, frequency, duration, timing and rate of change of flow (see Tharme 2003, Acreman and Dunbar 2004). For example, the Range of

Variability Approach uses Indicators of Hydrological Alteration (IHA) to define ecologically appropriate limits of hydrological change (Richter *et al.* 1996, 1997) and although it is usually applied to river flow it could, with appropriate modification, be employed to assess differences in baseline and scenario flood extent. Thompson *et al.* (2014b) employed the Ecological Risk due to Flow Alteration (ERFA) method (Laizé *et al.* 2014), a modified IHA approach in their assessment of GCM-related uncertainty for the Mekong. This risk-based method, which was based on the number of IHAs associated with both high and low flows that exceeded a specified threshold, could provide an initial assessment of the potential magnitude of ecological changes and their uncertainty across the Upper Niger (Thompson *et al.* 2017b). Development of the current study in this direction is the next obvious step for research into GCM-related uncertainty. It will, however, be important to recognize that there are other potential sources of uncertainty. These include modifications in response to climate change in current water management practices, including the operation of existing dams that are either included in the model or, in the case of the Talo Dam, not included since they were completed after the end of the simulation period. The potential for further investments in major hydraulic infrastructure throughout West Africa in response to growing demands for irrigation, domestic water supplies and hydropower has been identified (e.g. Barbier *et al.* 2009). A number of hydropower and irrigation projects are proposed for the Upper Niger (e.g. Hassane *et al.* 2000). New schemes, such as the Formi hydropower dam and another dam at Djenné on the Bani River, can be expected to modify river flow and, in turn, flood extent within the Inner Niger Delta (Zwarts *et al.* 2005a, Mahé *et al.* 2011a). It has, for example, been suggested that more than 55% of flows into the Delta in a wet year could be stored by existing and planned upstream dams (Liéno *et al.* 2010). Such flow reductions would offset the increases in discharge and hence flood extent projected by some GCMs and further increase the magnitude of the declines in river flow and, in particular, the area of inundation projected by many of the others. These changes will be compounded by modifications to water management, agricultural and other related policies that might occur in response to climate change and other pressures (e.g. Van Dijk *et al.* 2008). Similarly, further changes in land cover in response to climate change as well as anthropogenic activities, such as modifications to the extent of agricultural cultivation, represents another source of uncertainty. As discussed above, declines in natural Sahelian vegetation over recent decades have been widespread (e.g. Leblanc *et al.* 2008) and have been linked to increases in runoff coefficients (e.g.

Amogu *et al.* 2010, Liénoú *et al.* 2010). Continuation of such changes into the future could contribute to enhanced inflows to the Inner Niger Delta. The representation of such changes would most usefully be simulated using an alternative modelling approach that enables both spatially and temporally varying land cover (see Thompson *et al.* 2013, 2016).

Conclusions

A previously calibrated/validated hydrological model of the Upper Niger and the Inner Niger Delta has been used to investigate the impacts of RCP 4.5 scenarios for 41 CMIP5 GCMs and two future 30-year time slices centred on the 2050s and 2080s. Grouping of GCMs based on their genealogy was also undertaken to address independence of climate model results. Inter-GCM uncertainty in precipitation is substantially larger than uncertainty in PET. An almost equal number of the sub-catchment-GCM combinations project increases and decreases in mean annual precipitation. This is repeated for the genealogically-based GCM groups. Within individual sub-catchments, however, there is considerable variability in the number of GCMs projecting precipitation increases or decreases as well as the magnitude of the inter-GCM range in these changes. The 10–90-percentile range varies between 13.6 and 26.9% (mean: 19.0%) for the 2050s and 15.6 and 34.4% (mean 22.5%) for the 2080s. In contrast, all but 12 (2.4%) of the sub-catchment-GCM combinations project increases in annual PET. Declines are associated with the same sub-catchments, and two GCMs and are predominantly the result of projected declines in maximum temperature. Inter-GCM 10–90-percentile ranges of change vary between 3.8 and 4.8% (mean: 4.3%) for the 2050s and 4.5 and 6.4% (mean: 5.8%) for the 2080s. In percentage terms the ranges of change in precipitation for the 41 GCM ensemble and the 12 genealogically-based GCM groups are around four or five times as large as those of PET. These results are repeated for more central percentiles ranges. The 41 GCM ensemble mean scenario projects small changes in mean annual precipitation which vary in direction between sub-catchments (–2.0 to 6.3%), with more experiencing increases (eight and nine for the 2050s and 2080s, respectively). More sub-catchments experience small declines in the mean discharge for the group ensemble mean. Consistent increases in mean annual PET are projected by the ensemble mean. The magnitudes of these changes vary little between sub-catchments and are, on average, 4.0% for the 2050s and 5.0% the 2080s. Similar results are obtained for the group ensemble mean.

There is considerable uncertainty in projected river discharge with variations in both the direction and magnitude of changes in mean, low and high flows. Just over half of the 492 gauging station-GCM combinations experience increases in mean discharge for the 2050s, whilst just under half of these changes are positive for the 2080s. Inter-GCM ranges of change in discharge are two–three times as large as those for precipitation. As for precipitation, this range varies between gauging stations. For the 2050s the mean 10–90-percentile range is 52.9% and varies between 31.0% (–20.7 to 10.3%) and 75.8% (–32.7 to 43.1%). In common with precipitation and PET, inter-GCM ranges for discharge increase for the 2080s, with a mean of 59.5% and range between 30.5% (–20.1 to 10.3%) and 95.8% (–39.3 to 56.5%). Declines in mean discharge are dominant for the ensemble mean scenario (nine stations in both time slices) although they are relatively small, ranging between –11.5 and 4.0% (mean: –1.1%) for the 2050s and between –14.3 and 4.6% (mean: –2.2%) for the 2080s. Declines in mean discharge are projected at all stations for the group ensemble mean, but again they are small (mean: –7.3% for the 2050s, –8.7% for the 2080s).

Of the 41 GCMs, 25 (61%) project declines in mean annual river inflow to the Inner Niger Delta for the 2050s, the remainder suggesting that inflows will increase. Fewer GCMs (18 or 43%) project declines for the 2080s. An almost equal number of the 12 GCM groups project increases and decreases. Inter-GCM range of change for the 10–90-percentile range in the 2050s is 49.3% (–29.4 to 19.9%) and for the 2080s it is 48.2% (–27.9 to 20.3%), whilst the ensemble mean scenario is associated with small declines (–1.4 and –2.1%) for both time slices (with slightly larger increases for the group ensemble mean). More GCMs project declines in peak flood extent within the Inner Delta than those that suggest an increase in the extent of seasonal inundation. Mean flood extent during the peak months of October and November is projected to decline by 32 (78%) and 28 (68%) of GCMs in the 2050s and 2080s, respectively. Far more GCMs project declines in all or the majority of annual peak flood extents within the 30-year simulation periods compared to those that project consistent or near consistent increases. For the 2050s, when 33 GCMs project declines in all of the annual peaks, changes in the mean of these peaks for the 10–90-percentile range from –6136 km² (–43.0%) to 987 km² (6.9%) compared to the baseline 14 258 km². The ensemble mean projects a decline of 1870 km² (13.1, 19.5% for the group ensemble mean). In the 2080s, declines in all annual peaks are projected by 26 GCMs, whilst the

10–90-percentile range of change in the mean annual peak is -6176 km^2 (-43.3%) to 1165 km^2 (8.2%). A decline of 2076 km^2 (14.6%) is projected by the ensemble mean (20.9% for the group ensemble mean). Many GCMs project increases in the extent of surface water that remains within the Inner Niger Delta during the dry season. With a few exceptions, these increases are, however, small in absolute terms.

This study has focused on evaluating the hydrological impacts and associated uncertainty of projected changes in climate. Assessment of the potential risks of ecological changes that could result from modifications to river regimes using environmental flow approaches would be a logical extension. Modification of these approaches to enable comparisons of baseline and projected flood extent could provide a means of inferring likely ecological impacts of changes in inundation within the Inner Niger Delta. Other sources of uncertainty could also be considered through modification of the model to include new and proposed water management infrastructure, in particular dams, enabling their impacts under current and potential future climate to be assessed. Further uncertainty regarding hydrological conditions in the Upper Niger and the Inner Niger Delta is inevitably linked to future changes in land cover as well as water management and related policies that may be driven, at least in part, by a changing climate and its hydrological consequences.

Acknowledgements

The present study develops earlier research funded by a grant from the UK Natural Environmental Research Council under the Quantifying and Understanding the Earth System (QUEST) programme (Ref. NE/E001890/1). The paper benefitted from discussions with Chris Brierley and Joon Ho (UCL Geography). Two anonymous reviewers provided useful comments on an earlier draft.

Disclosure statement

No potential conflict of interest was reported by the authors.

Funding

This work was supported by the Natural Environment Research Council [NE/E001890/1].

References

Abramowitz, G., 2010. Model independence in multi-model ensemble prediction. *Australian Meteorological and Oceanographic Journal*, 59, 3–6. doi:10.22499/2.00000

- Acreman, M.C., *et al.*, 2009. A simple framework for evaluating regional wetland ecohydrological response to climate change with case studies from Great Britain. *Ecohydrology*, 2, 1–17. doi:10.1002/eco.v2:1
- Acreman, M.C. and Dunbar, M.J., 2004. Defining environmental river flow requirements – a review. *Hydrology and Earth System Sciences*, 8, 861–876. doi:10.5194/hess-8-861-2004
- Adams, W.M., 1992. *Wasting the rain: rivers, people and planning in Africa*. London: Earthscan.
- Amogu, O., *et al.*, 2010. Increasing river flows in the Sahel? *Water*, 2, 170–199. doi:10.3390/w2020170
- Anandhi, A., *et al.*, 2011. Examination of change factor methodologies for climate change impact assessment. *Water Resources Research*, 47, W03501. doi:10.1029/2010WR009104
- Ardoin-Bardin, A., *et al.*, 2009. Using general circulation model outputs to assess impacts of climate change on runoff for large hydrological catchments in West Africa. *Hydrological Sciences Journal*, 54, 77–89. doi:10.1623/hysj.54.1.77
- Arnell, N.W. and Gosling, S.N., 2013. The impacts of climate change on river flow regimes at the global scale. *Journal of Hydrology*, 486, 351–364. doi:10.1016/j.jhydrol.2013.02.010
- Baker, C., Thompson, J.R., and Simpson, M., 2009. Hydrological dynamics I: surface waters, flood and sediment dynamics. In: E.B. Maltby and T. Barker, eds. *The wetlands handbook*. Chichester: Wiley-Blackwells, 120–168.
- Barbier, B., *et al.*, 2009. Le retour des grands investissements hydrauliques en Afrique de l'Ouest: les perspectives et les enjeux. *Geocarrefour*, 84, 31–41. doi:10.4000/geocarrefour.7205
- Barbier, E.B. and Thompson, J.R., 1998. The value of water: floodplain versus large-scale irrigation benefits in northern Nigeria. *Ambio*, 27, 434–440.
- Barron, O., *et al.*, 2012. Climate change effects on water-dependent ecosystems in south-western Australia. *Journal of Hydrology*, 434, 95–109. doi:10.1016/j.jhydrol.2012.02.028
- Bates, B.C., *et al.*, eds. 2008. *Climate change and water*. Technical paper of the Intergovernmental Panel on Climate Change. Geneva: IPCC Secretariat.
- Beadle, L.C., 1974. *The inland waters of tropical Africa: an introduction to tropical limnology*. London: Longman.
- Bergé-Nguyen, M. and Crétaux, J.C., 2015. Inundations in the Inner Niger Delta: monitoring and analysis using MODIS and global precipitation datasets. *Remote Sensing*, 2015 (7), 2127–2151. doi:10.3390/rs70202127
- Blaser, W.J., 2013. *Impact of woody encroachment on soil-plant-herbivore interactions in the Kafue Flats floodplain ecosystem*. Thesis (PhD). Zurich: ETH Zurich.
- Bureau, R., 2002. *Climate change and Wetlands: impacts, adaptations and mitigation*. Ramsar COP8 DOC.11. Gland: Ramsar Convention Bureau.
- Candela, L., *et al.*, 2009. Impact assessment of combined climate and management scenarios on groundwater resources and associated wetland (Majorca, Spain). *Journal of Hydrology*, 376, 510–527. doi:10.1016/j.jhydrol.2009.07.057
- Carroll, M.J., *et al.*, 2015. Hydrologically driven ecosystem processes determine the distribution and persistence of ecosystem-specialist predators under climate change. *Nature Communications*, 6, 7851. doi:10.1038/ncomms8851
- Chiew, F.H.S., *et al.*, 2008. *Rainfall-runoff modelling across the Murray-Darling Basin*. A report to the Australian

- Government from the CSIRO Murray-Darling Basin Sustainable Yields Project. Canberra: CSIRO.
- Clilverd, H.M., *et al.*, 2016. Coupled hydrological/hydraulic modelling of river restoration impacts and floodplain hydrodynamics. *River Research and Applications*, 32, 1927–1948. doi:10.1002/rra.v32.9
- Crétaux, J.C., *et al.*, 2011. Flood mapping inferred from remote sensing data. *International Water Technology Journal*, 1, 46–58.
- Dai, A., 2012. Increasing drought under global warming in observations and models. *Nature Climate Change*, 3, 52–58. doi:10.1038/nclimate1633
- Descroix, L., *et al.*, 2009. Spatio-temporal variability of hydrological regimes around the boundaries between Sahelian and Sudanian areas of West Africa: a synthesis. *Journal of Hydrology*, 375, 90–102. doi:10.1016/j.jhydrol.2008.12.012
- Diaz-Nieto, J. and Wilby, R., 2005. A comparison of statistical downscaling and climate change factor methods: impacts on low flows in the River Thames, United Kingdom. *Climatic Change*, 69, 245–268. doi:10.1007/s10584-005-1157-6
- Diello, P., *et al.*, 2005. Relationship between rainfall and vegetation indexes in Burkina Faso: a case study of the Nakambé Basin. *Hydrological Sciences Journal*, 50, 207–221. doi:10.1623/hysj.50.2.207.61797
- Drijver, C.A. and Marchand, M., 1985. *Taming the floods: environmental aspects of floodplain development in Africa*. Leiden: Centre for Environmental Studies, University of Leiden.
- Dyson, M., Bergkamp, G., and Scanlon, J., eds., 2003. *Flow - the essentials of environmental flows*. Gland: IUCN.
- Erwin, K.L., 2009. Wetlands and global climate change: the role of wetland restoration in a changing world. *Wetlands Ecology and Management*, 17, 71–84. doi:10.1007/s11273-008-9119-1
- Farquharson, F., 2007. The deterioration in hydrometric data collection in Africa; what can be done about it? In: *Earth: our Changing Planet. Proceedings of the International Union of Geodesy and Geophysics XXIV General Assembly* [online], 2–13 July. Perugia: International Union of Geodesy and Geophysics. Available from: http://www.wmo.int/pages/prog/hwrrp/documents/WMO-IAHS_knowledge.pdf
- Gasca-Tucker, D.L., *et al.*, 2007. Estimating evaporation from a wet grassland. *Hydrology and Earth System Sciences*, 11, 270–282. doi:10.5194/hess-11-270-2007
- Ghosh, S. and Mujumdar, P.P., 2009. Climate change impact assessment: uncertainty modelling with imprecise probability. *Journal of Geophysical Research*, 114, D18113. doi:10.1029/2008JD011648
- Giles, J., 2005. Solving Africa's climate data problem. *Nature*, 435, 863.
- Gillett, N.P., *et al.*, 2002. Detecting anthropogenic influence with a multi-model ensemble. *Geophysical Research Letters*, 29, 1970. doi:10.1029/2002GL015836
- Goes, B.J.M., 2002. Effects of river regulation on aquatic macrophyte growth and floods in the Hadejia-Nguru Wetlands and flow in the Yobe River, northern Nigeria; implications for future water management. *River Research and Applications*, 18, 81–95. doi:10.1002/(ISSN)1535-1467
- Goosen, H. and Kone, B., 2005. Livestock in the Inner Niger Delta. In: L. Zwarts, *et al.*, eds. *The Niger, a lifeline: effective water management in the Upper Niger Basin*. Lelystad: RIZA, 121–135.
- Gosling, S.N., *et al.*, 2011. A comparative analysis of projected impacts of climate change on river runoff from global and catchment-scale hydrological models. *Hydrology and Earth System Sciences*, 15, 279–294. doi:10.5194/hess-15-279-2011
- Gosling, S.N. and Arnell, N.W., 2011. Simulating current global river runoff with a global hydrological model: model revisions, validation and sensitivity analysis. *Hydrological Processes*, 25, 1129–1145. doi:10.1002/hyp.v25.7
- Graham, L.P., Andréasson, J., and Carlsson, B., 2007. Assessing climate change impacts on hydrology from an ensemble of regional climate models, model scales and linking methods – a case study on the Lule River basin. *Climatic Change*, 81, 293–307. doi:10.1007/s10584-006-9215-2
- Green, A.J., *et al.*, 2014. Quantifying the relative magnitude of sources of uncertainty in river flow projections under climate change: an assessment for the Mekong River. *European Geosciences Union General Assembly 2014 Abstracts* (EGU2014-15019).
- Grove, A.T., ed., 1985. *The Niger and its neighbours: environmental history and hydrobiology, human use and health hazards of the major West African rivers*. Rotterdam: Balkema.
- Haddeland, I., *et al.*, 2011. Multi-model estimate of the global water balance: setup and first results. *Journal of Hydrometeorology*, 12, 869–884. doi:10.1175/2011JHM1324.1
- Hanel, M. and Buishand, T.A., 2015. Assessment of the sources of variation in changes of precipitation characteristics over the Rhine Basin using a linear mixed-effects model. *Journal of Climate*, 28, 6903–6919. doi:10.1175/JCLI-D-14-00775.1
- Hargreaves, G.H. and Samani, Z.A., 1982. Estimating potential evapotranspiration. *Journal of the Irrigation and Drainage Division, American Society of Civil Engineers*, 108, 225–230.
- Hassane, A., Kuper, M., and Orange, D., 2000. Influence des aménagements hydrauliques et hydro-agricoles du Niger supérieur sur l'onde de la crue du delta intérieur du Niger au Mali. *Sud Sciences & Technologies*, 5, 16–31.
- Henriksen, H.J., *et al.*, 2003. Methodology for construction, calibration and validation of a national hydrological model for Denmark. *Journal of Hydrology*, 280, 52–71. doi:10.1016/S0022-1694(03)00186-0
- Henriksen, H.J., *et al.*, 2008. Assessment of exploitable groundwater resources of Denmark by use of ensemble resource indicators and a numerical groundwater–surface water model. *Journal of Hydrology*, 348, 224–240. doi:10.1016/j.jhydrol.2007.09.056
- Hirabayashi, Y., *et al.*, 2013. Global flood risk under climate change. *Nature Climate Change*, 3, 816–821. doi:10.1038/NCLIMATE1911
- Ho, J.T., Thompson, J.R., and Brierley, C., 2016. Projections of hydrology in the Tocantins-Araguaia Basin, Brazil: uncertainty assessment using the CMIP5 ensemble. *Hydrological Sciences Journal*, 61, 551–567. doi:10.1080/02626667.2015.1057513
- Hollis, G.E. and Thompson, J.R., 1993a. Hydrological model of the floodplain. In: G.E. Hollis, W.M. Adams, and M. Aminu-Kano, eds. *The Hadejia Nguru Wetlands:*

- environment, economy and sustainable development of a Sahelian floodplain wetland*. Gland: IUCN, 69–80.
- Hollis, G.E. and Thompson, J.R., 1993b. Water resource developments and their hydrological impacts. In: G.E. Hollis, W.M. Adams, and M. Aminu-Kano, eds. *The Hadejia Nguru Wetlands: environment, economy and sustainable development of a Sahelian floodplain wetland*. Gland: IUCN, 149–190.
- House, A.R., Thompson, J.R., and Acreman, M.C., 2016. Projecting impacts of climate change on a chalk valley riparian wetland. *Journal of Hydrology*, 534, 178–192. doi:10.1016/j.jhydrol.2016.01.004
- IPCC (Intergovernmental Panel on Climate Change). 2014. *Climate change 2014: synthesis report*. Contribution of Working Groups I, II and III to the fifth assessment report of the Intergovernmental Panel on Climate Change. Geneva: IPCC.
- John, D.M., Lévêque, C., and Newton, L.E., 1993. Western Africa. In: D.F. Whigham, D. Dykyjová, and S. Hejný, eds. *Wetlands of the world: inventory, ecology and management*. Vol. 1. Dordrecht: Kluwer, 47–78.
- Kingsford, R.T., Lemly, A.D., and Thompson, J.R., 2006. Impacts of dams, river management and diversions on desert rivers. In: R.T. Kingsford, ed. *Ecology of desert rivers*. Cambridge: Cambridge University Press, 203–247.
- Kingston, D.G. and Taylor, R.G., 2010. Sources of uncertainty in climate change impacts on river discharge and groundwater in a headwater catchment of the Upper Nile Basin, Uganda. *Hydrology and Earth System Science*, 14, 1297–1308. doi:10.5194/hess-14-1297-2010
- Kingston, D.G., Thompson, J.R., and Kite, G., 2011. Uncertainty in climate change projections of discharge for the Mekong River Basin. *Hydrology and Earth System Science*, 15, 1459–1471. doi:10.5194/hess-15-1459-2011
- Knutti, R., et al., 2009. Challenges in combining projections from multiple climate models. *Journal of Climate*, 23, 2739–2758. doi:10.1175/2009JCLI3361.1
- Knutti, R., Masson, D., and Gettelman, A., 2013. Climate model genealogy: generation CMIP5 and how we got there. *Geophysical Research Letters*, 40, 1194–1199. doi:10.1002/grl.50256
- Knutti, R. and Sedlacek, J., 2013. Robustness and uncertainties in the new CMIP5 climate model projections. *Nature Climate Change*, 3, 369–373. doi:10.1038/nclimate1716
- Koirala, S., et al., 2014. Global assessment of agreement among streamflow projections using CMIP5 model outputs. *Environmental Research Letters*, 9, 064017. doi:10.1088/1748-9326/9/6/064017
- Kundzewicz, Z.W., et al., 2007. Freshwater resources and their management. In: M.L. Parry, et al., eds. *Climate change 2007: impacts, adaptation and vulnerability*. Contribution of Working Group II to the Fourth Assessment Report of the Intergovernmental Panel on Climate Change. Cambridge: Cambridge University Press, 173–210.
- Laizé, C.L.R., et al., 2014. Projected flow alteration and ecological risk for pan-European rivers. *River Research and Applications*, 30, 299–314. doi:10.1002/rra.v30.3
- Lambert, S.J. and Boer, G.J., 2001. CMIP1 evaluation and intercomparison of coupled climate models. *Climate Dynamics*, 17, 83–106. doi:10.1007/PL00013736
- Leblanc, M., et al., 2008. Land clearance and hydrological change in the Sahel: SW Niger. *Global Planetary Change*, 61, 49–62. doi:10.1016/j.gloplacha.2007.08.011
- Lemly, A.D., Kingsford, R.T., and Thompson, J.R., 2000. Irrigated agriculture and wildlife conservation: conflict on a global scale. *Environmental Management*, 25, 485–512. doi:10.1007/s002679910039
- Liéno, G., et al., 2005. Regimes of suspended sediment flux in Cameroon: review and synthesis for the main ecosystems; climatic diversity and anthropogenic activities. *Hydrological Sciences Journal*, 50, 111–123. doi:10.1623/hysj.50.1.111.56329
- Liéno, G., et al., 2010. The River Niger water availability: facing future needs and climate change. In: E. Servat, S. Demuth, A. Dezetter, and T. Daniell, eds. *Global change: facing risks and threats to water resources*, (Proceedings of the Sixth World FRIEND Conference, Fez, Morocco, October 2010). Wallingford: IAHS Publication 340, 637–645.
- Louvet, S., et al., 2011. Variabilité spatio-temporelle passée et future de la pluie sur le bassin du Bani en Afrique de l'Ouest. In: S. Franks, E. Boegh, E. Blyth, D.M. Hannah, and K.K. Yilmaz, eds. *Hydro-climatology: variability and change*, (Proceedings of symposium J-H02 held during IUGG2011 in Melbourne, Australia, July 2011). Wallingford: IAHS Publication 344, 125–130.
- Mahé, G., 2009. Surface/groundwater interactions in the Bani and Nakambe rivers, tributaries of the Niger and Volta basins, West Africa. *Hydrological Sciences Journal*, 61, 704–712. doi:10.1623/hysj.54.4.704
- Mahé, G., et al., 2009. Water losses in the inner delta of the River Niger: water balance and flooded area. *Hydrological Processes*, 23, 3157–3160. doi:10.1002/hyp.v23:22
- Mahé, G., et al., 2011a. Le fleuve Niger et le changement climatique au cours des 100 dernières années. In: S. Franks, E. Boegh, E. Blyth, D.M. Hannah, and K.K. Yilmaz, eds. *Hydro-climatology: variability and change*, (Proceedings of symposium J-H02 held during IUGG2011 in Melbourne, Australia, July 2011). Wallingford: IAHS Publication 344, 131–137.
- Mahé, G., et al., 2011b. Estimation of the flooded area of the Inner Delta of the River Niger in Mali by hydrological balance and satellite data. In: S. Franks, E. Boegh, E. Blyth, D.M. Hannah, and K.K. Yilmaz, eds. *Hydro-climatology: variability and change*, (Proceedings of symposium J-H02 held during IUGG2011 in Melbourne, Australia, July 2011). Wallingford: IAHS Publication 344, 138–143.
- Maltby, E.B., et al., 2011. Freshwaters – openwaters, wetlands and floodplains. In: *The UK National Ecosystem Assessment Technical Report, UK National Ecosystem Assessment* [online]. Cambridge: UNEP-WCMC, 295–360. Available from: <http://uknea.unep-wcmc.org/Resources/tabid/82/Default.aspx>
- Mariko, A., 2004. *Caractérisation et suivi de la dynamique de l'inondation et du couvert végétal dans le Delta Intérieur du Niger (Mali) par télédétection*. Thesis (PhD). Montpellier: Université Montpellier 2.
- Mariko, A., Mahé, G., and Servat, E., 2003. Les surfaces inondées dans le Delta Intérieur du Niger. *Bulletin SFPT*, 172, 61–68.
- Masson, D. and Knutti, R., 2011. Climate model genealogy. *Geophysical Research Letters*, 38, L08703. doi:10.1029/2011GL046864
- Maxino, C.C., et al., 2008. Ranking the AR4 climate models over the Murray-Darling Basin using simulated maximum temperature, minimum temperature and precipitation. *International Journal of Climatology*, 28, 1097–1112. doi:10.1002/joc.1612

- Meynell, P.J., *et al.*, 2012. An integrated fire and water management strategy using the ecosystem approach: tram Chim National Park, Vietnam. *In*: E.R.N. Gunawardena, B. Gopal, and H.B. Kotagama, eds. *Ecosystems and integrated water resources management in South Asia*. New Delhi: Routledge, 199–228.
- Mitchell, T.D. and Jones, P.D., 2005. An improved method of constructing a database of monthly climate observations and associated high-resolution grids. *International Journal of Climatology*, 25, 693–712. doi:10.1002/(ISSN)1097-0088
- Moss, R.H., *et al.*, 2010. The next generation of scenarios for climate change research and assessment. *Nature*, 463, 747–756. doi:10.1038/nature08823
- Mumba, M. and Thompson, J.R., 2005. Hydrological and ecological impacts of dams on the Kafue Flats floodplain system, southern Zambia. *Physics and Chemistry of the Earth*, 30, 442–447. doi:10.1016/j.pce.2005.06.009
- Nash, I.E. and Sutcliffe, I.V., 1970. River flow forecasting through conceptual models. *Journal of Hydrology*, 10, 282–290. doi:10.1016/0022-1694(70)90255-6
- Nestler, J.M., *et al.*, 2012. The river machine: A template for fish movement and habitat, fluvial geomorphology, fluid dynamics and biogeochemical cycling. *River Research and Applications*, 28, 490–503. doi:10.1002/rra.1567
- Palmer, T., *et al.*, 2005. Probabilistic prediction of climate using multi-model ensembles: from basics to applications. *Philosophical Transactions of the Royal Society B: Biological Sciences*, 360, 1991–1998. doi:10.1098/rstb.2005.1750
- Perkins, S.E., *et al.*, 2007. Evaluation of the AR4 climate models' simulated daily maximum temperature, minimum temperature and precipitation over Australia using probability density functions. *Journal of Climate*, 20, 4356–4376. doi:10.1175/JCLI4253.1
- Pirtle, Z., Meyer, R., and Hamilton, A., 2010. What does it mean when climate models agree? A case for assessing independence among general circulation models. *Environmental Science & Policy*, 13, 351–361. doi:10.1016/j.envsci.2010.04.004
- Pitman, W.V., 2011. Overview of water resource assessment in South Africa: current state and future challenges. *Water SA*, 37, 659–664. doi:10.4314/wsa.v37i5.3
- Poff, N.L., *et al.*, 1997. The natural flow regime: a new paradigm for riverine conservation and restoration. *BioScience*, 47, 769–784. doi:10.2307/1313099
- Polet, G. and Thompson, J.R., 1996. Maintaining the floods - hydrological and institutional aspects of managing the Komadugu-Yobe basin and its floodplain wetlands. *In*: M.C. Acreman and G.E. Hollis, eds. *Water management and wetlands in Sub-Saharan Africa*. Gland: IUCN, 73–90.
- Prudhomme, C. and Davies, H., 2009. Assessing uncertainties in climate change impact analyses on the river flow regimes in the UK. Part 1: baseline climate. *Climatic Change*, 93, 177–195. doi:10.1007/s10584-008-9464-3
- Rebello, L.-M., McCartney, M.P., and Finlayson, C.M., 2010. Wetlands of Sub-Saharan Africa: distribution and contribution of agriculture to livelihoods. *Wetlands Ecology and Management*, 18, 557–572. doi:10.1007/s11273-009-9142-x
- Richter, B.D., *et al.*, 1996. A method for assessing hydrologic alteration within ecosystems. *Conservation Biology*, 10, 1163–1174. doi:10.1046/j.1523-1739.1996.10041163.x
- Richter, B.D., *et al.*, 1997. How much water does a river need? *Freshwater Biology*, 37, 231–249. doi:10.1046/j.1365-2427.1997.00153.x
- Robinson, A.J. 2017. *Uncertainty in hydrological scenario modelling: an investigation using the Mekong River Basin, SE Asia*. Thesis (PhD). London: UCL (University College London).
- Schneider, S.H., 1983. CO₂, climate and society: a brief overview. *In*: R. Chen, E. Boulding, and S. Schneider, eds. *Social science research and climate change: an interdisciplinary appraisal*. Dordrecht: Springer, 9–15.
- Scoones, I., 1991. Wetlands in drylands: key resources for agricultural and pastoral production in Africa. *Ambio*, 20, 366–371.
- Singh, C.R., *et al.*, 2010. Modelling the impact of prescribed global warming on runoff from headwater catchments of the Irrawaddy River and their implications for the water level regime of Loktak Lake, northeast India. *Hydrology and Earth System Science*, 14, 1745–1765. doi:10.5194/hess-14-1745-2010
- Singh, C.R., *et al.*, 2011. Modelling water-level options for ecosystem services and assessment of climate change: loktak Lake, northeast India. *Hydrological Sciences Journal*, 56, 1518–1542. doi:10.1080/02626667.2011.631012
- Sutcliffe, J.V. and Parks, Y.P., 1987. Hydrological modelling of the Sudd and Jonglei Canal. *Hydrological Sciences Journal*, 32, 143–159. doi:10.1080/02626668709491174
- Sutcliffe, J.V. and Parks, Y.P., 1989. Comparative water balances of selected African wetlands. *Hydrological Sciences Journal*, 34, 49–62. doi:10.1080/02626668909491308
- Tebaldi, C. and Knutti, R., 2007. The use of the multi-model ensemble in probabilistic climate projections. *Philosophical Transactions of the Royal Society A: Mathematical, Physical and Engineering Sciences*, 365, 2053–2075. doi:10.1098/rsta.2007.2076
- Tharme, R.E., 2003. A global perspective on environmental flow assessment: emerging trends in the development and application of environmental flow methodologies for rivers. *River Research and Applications*, 19, 397–441. doi:10.1002/(ISSN)1535-1467
- Thompson, J.R., 1995. *Hydrology, Water Management and Wetlands of the Hadejia Jama'are Basin, Northern Nigeria*. Thesis (PhD). London: University of London.
- Thompson, J.R., *et al.*, 2009. Modelling the hydrological impacts of climate change on UK lowland wet grassland. *Wetlands Ecology and Management*, 17, 503–523. doi:10.1007/s11273-008-9127-1
- Thompson, J.R., 2012. Modelling the impacts of climate change on upland catchments in southwest Scotland using MIKE SHE and the UKCP09 probabilistic projections. *Hydrology Research*, 43, 507–530. doi:10.2166/nh.2012.105
- Thompson, J.R., *et al.*, 2013. Assessment of uncertainty in river flow projections for the Mekong River using multiple GCMs and hydrological models. *Journal of Hydrology*, 466, 1–30. doi:10.1016/j.jhydrol.2013.01.029
- Thompson, J.R., *et al.*, 2014b. Climate change uncertainty in environmental flows for the Mekong River. *Hydrological Sciences Journal*, 59, 259–279. doi:10.1080/02626667.2013.842074
- Thompson, J.R., *et al.*, 2017a. Simulation of the hydrological impacts of climate change on a restored floodplain. *Hydrological Sciences Journal*, 62. doi:10.1080/02626667.2017.1390316

- Thompson, J.R., *et al.* 2017b. GCM-related uncertainty in future environmental flows and flooding in the Upper Niger and Inner Niger Delta. *International Association of Hydrological Sciences 2017 Scientific Assembly Abstracts* (IAHS2017-362). Wallingford: IAHS Press. Available from: <http://meetingorganizer.copernicus.org/IAHS2017/IAHS2017-362-1.pdf>
- Thompson, J.R., Crawley, A., and Kingston, D.G., 2016. GCM-related uncertainty for river flows and inundation under climate change: the Inner Niger Delta. *Hydrological Sciences Journal*, 61, 2325–2347. doi:10.1080/02626667.2015.1117173
- Thompson, J.R., Green, A.J., and Kingston, D.G., 2014a. Potential evapotranspiration-related uncertainty in climate change impacts on river flow: an assessment for the Mekong River basin. *Journal of Hydrology*, 510, 259–279. doi:10.1016/j.jhydrol.2013.12.010
- Thompson, J.R. and Hollis, G.E., 1995. Hydrological modelling and the sustainable development of the Hadejia-Nguru Wetlands, Nigeria. *Hydrological Sciences Journal*, 40, 97–116. doi:10.1080/02626669509491393
- Thompson, J.R., 1996. Africa's floodplains: a hydrological overview. In: M.C. Acreman and G.E. Hollis, eds. *Water management and wetlands in Sub-Saharan Africa*. Gland: IUCN, 5–20.
- Thompson, J.R. and Polet, G., 2000. Hydrology and land use in a Sahelian floodplain wetland. *Wetlands*, 20, 639–659. doi:10.1672/0277-5212(2000)020[0639:HALUIA]2.0.CO;2
- Thomson, A.M., *et al.*, 2011. RCP4.5: a pathway for stabilization of radiative forcing by 2100. *Climatic Change*, 109, 77–94. doi:10.1007/s10584-011-0151-4
- Trouet, V. and Van Oldenborgh, G.J., 2013. KNMI climate explorer: a web-based research tool for high-resolution paleoclimatology. *Tree-Ring Research*, 69, 3–13. doi:10.3959/1536-1098-69.1.3
- Van der Kamp, J., Fofana, B., and Wymenga, E., 2005. Ecological values of the Inner Niger Delta. In: L. Zwarts, *et al.*, eds. *The Niger, a lifeline: effective water management in the Upper Niger Basin*. RIZA: Wetlands International, 155–176.
- Van Dijk, A.I.J.M., *et al.*, 2008. *Uncertainty in river modelling across the Murray-Darling Basin*. A report to the Australian Government from the CSIRO Murray-Darling Basin Sustainable Yields Project, Canberra: CSIRO.
- van Vuuren, D.P., *et al.*, 2011. The representative concentration pathways: an overview. *Climatic Change*, 109, 5–31. doi:10.1007/s10584-011-0148-z
- Voinov, A., *et al.*, 2007. Patuxent landscape model: 1. hydrological model development. *Water Resources*, 34, 163–170. doi:10.1134/S0097807807020066
- Welcomme, R.L., 1986. Fish of the Niger system. In: B.R. Davies and K.F. Walker, eds. *The ecology of river systems*. Dordrecht: Junk, 25–47.
- Wilby, R.L. and Dessai, S., 2010. Robust adaptation to climate change. *Weather*, 65, 180–185. doi:10.1002/wea.v65:7
- Wilby, R.L. and Wigley, T.M.L., 1997. Downscaling general circulation model output: a review of methods and limitations. *Progress in Physical Geography*, 21, 530–548. doi:10.1177/030913339702100403
- Willems, P., *et al.*, 2012. *Impacts of climate change on rainfall extremes and urban drainage systems*. London: IWA Publishing.
- World Bank, United Nations Environment Programme, African Development Bank, French Ministry of Cooperation and European Community. 1993. *Sub-Saharan Africa hydrological assessment*. Washington, DC: World Bank.
- Zhang, L. and Mitsch, W.J., 2005. Modelling hydrological processes in created freshwater wetlands: an integrated system approach. *Environmental Modelling & Software*, 20, 935–946. doi:10.1016/j.envsoft.2004.03.020
- Zwarts, L., Cisse, N., and Diallo, M., 2005a. Hydrology of the Upper Niger. In: L. Zwarts, *et al.*, eds. *The Niger, a lifeline: effective water management in the Upper Niger Basin*. Riza: Wetlands International, 15–41.
- Zwarts, L. and Diallo, M., 2005. Fisheries in the Inner Niger Delta. In: L. Zwarts, *et al.*, eds. *The Niger, a lifeline: effective water management in the Upper Niger Basin*. Riza: Wetlands International, 89–107.
- Zwarts, L., Grigoras, I., and Hanganu, J., 2005b. Vegetation of the lower inundation zone of the Inner Delta. In: L. Zwarts, *et al.*, eds. *The Niger, a lifeline: effective water management in the Upper Niger Basin*. Riza: Wetlands International, 109–119.
- Zwarts, L. and Grigoras, I., 2005. Flooding of the Inner Niger Delta. In: L. Zwarts, *et al.*, eds. *The Niger, a lifeline: effective water management in the Upper Niger Basin*. RIZA: Wetlands International, 43–77.
- Zwarts, L. and Kone, B., 2005a. People in the Inner Niger Delta. In: L. Zwarts, *et al.*, eds. *The Niger, a lifeline: effective water management in the Upper Niger Basin*. Riza: Wetlands International, 79–86.
- Zwarts, L. and Kone, B., 2005b. Rice production in the Inner Niger Delta. In: L. Zwarts, *et al.*, eds. *The Niger, a lifeline: effective water management in the Upper Niger Basin*. Riza: Wetlands International, 137–153.